The evolution of the westernmost Mediterranean basins

Laura Gómez de la Peña, César R. Ranero, Eulàlia Gràcia, Guillermo Booth-Rea

PII: S0012-8252(20)30491-8

DOI: https://doi.org/10.1016/j.earscirev.2020.103445

Reference: EARTH 103445

To appear in: *Earth-Science Reviews*

Received date: 1 December 2019

Revised date: 13 November 2020

Accepted date: 18 November 2020

Please cite this article as: L.G. de la Peña, C.R. Ranero, E. Gràcia, et al., The evolution of the westernmost Mediterranean basins, *Earth-Science Reviews* (2020), https://doi.org/10.1016/j.earscirev.2020.103445

The evolution of the westernmost Mediterranean basins

Laura Gómez de la Peña[1*], César R. Ranero[1,2], Eulàlia Gràcia[1] and Guillermo Booth-Rea[3,4]

[1]*Barcelona Center for Subsurface Imaging, Institut de Ciències del Mar, CSIC, 08003 Barcelona, Spain*

[2]*Institució Catalana de Recerca i Estudis Avançats (ICREA), Passeig Lluis Companys 23, 08010 Barcelona, Spain*

[3]*Facultad de Ciencias, Universidad de Granada, 18071 Granada, Spain*

[4]*Instituto Andaluz de Ciencias de la Tierra, CSIC, Granada, Spain*

**Now at: GEOMAR Helmholtz Centre for Ocean Research Kiel, 24148 Kiel, Germany*

Corresponding author: Laura Gómez de la Peña (lgomez@geomar.de)

GEOMAR Helmholtz Centre of Ocean Research Kiel

Wischhofstr. 1-3, 24148 Kiel, Germany

Highlights:

- We present the first unified stratigraphy of the westernmost Mediterranean.
- Miocene marine basins currently onshore are integrated.
- We present a kinematic model for the Alboran and Algero-Balearic basins.
- We evaluate western Mediterranean geodynamic models in the framework of basin evolution.

1. Introduction

The formation of the Western Mediterranean Basins began in the Oligocene as a result of the migration/dispersal of the Alboran, Kabylies, Peloritan and Corsica-Sardinia-Calabria (AlKaPeCa, inset Fig. 1) terranes/microplates along with a contemporaneous subduction of the Tethys lithosphere (Rehault et al., 1984). The Alboran and Algero-Balearic basins are the westernmost of these basins, extending between North Africa and Iberia (inset Fig. 1a). During most of its history, the region contained several depocenters that have usually been individually studied, and described in the literature as basins; while here we describe them as sub-basins. There are six main historically described offshore sub-basins: the West Alboran Basin (WAB), the Malaga Basin (MB), the South Alboran Basin (SAB), the Pytheas Basin (PB), the Habibas Basin (HBB), and the East Alboran Basin (EAB) that joins eastward to the Algero-Balearic Basin (ABB) (Fig. 1a). There are also ten main onshore sub-basins, named Fortuna, Lorca, Mazarrón, Vera, Tabernas-Sorbas, Níjar, Baza, Guadix, Granada and Malaga (Fig. 1b). The tectonic structure and sedimentary infill of these sub-basins record key information to understand their formation processes and appraise geodynamic models of the western Mediterranean.

However, the stratigraphy and tectonic studies of different offshore and onshore sub-basins have not been integrated in a single comprehensive study. Previous works have resulted in a suite of different models for each area, with interpretations that are not fully compatible when compared among the sub-basins. This hinders the understanding of regional-scale formation processes and the evaluation of geodynamic evolution models of the western Mediterranean.

In this study, we review and update the seismic stratigraphy of the westernmost Mediterranean, including all Alboran sub-basins, the western ABB and emerged sub-basins in the Betics, focusing on the Neogene and Quaternary sedimentary units. We present a modern seismic dataset collected and processed by the Barcelona Center for Subsurface imaging that covers the entire system, providing correlation across sub-basins to define a coherent stratigraphy for the entire region. These results are used to evaluate existing models of basin formation and geodynamic evolution. Our main objectives are: (1) to define a coherent seismostratigraphic framework for the entire region, integrating previous interpretations and available well-data information to establish a correlation between the units of different sub-basins; (2) to interpret the sedimentary record of the main depocenters to propose an evolutionary model that accounts for each sub-basin; (3) to evaluate existing geodynamic models of the westernmost Mediterranean; and (4) to integrate the results in a coherent evolutionary model for the entire region.

2. Geological setting

The western Mediterranean formed in a context of NW-SE plate convergence between the African and Eurasian plates (Dewey et al., 1989), with the driving forces having an important contribution from slab dynamics in the mantle, acting obliquely to the NW-SE plate convergence (Lonergan and White, 1997; Carminati et al., 1998; Wortel and Spakman, 2000; Faccenna et al., 2004). The interaction between plate convergence and mantle-driven mechanisms produced compressional and extensional domains that migrated in space and time during the Cenozoic. Geodynamic interaction in the western Mediterranean involved also a set of small plates, such as the Iberian and Apulian plates, and the AlKaPeCa allochthonous meso-Mediterranean metamorphic terrains (Boullin et al., 1986, van Hinsbergen et al., 2020).

The structure of the resulting extensional basins is complex, their evolutionary histories are distinct and diverse and not well explored by modern studies. The Ligurian and Tyrrhenian basins (inset Fig. 1a) opened by rollback of the Ionian slab, leading to break-up of the Variscan lithosphere. The Ligurian and Tyrrhenian break-ups were followed by local magmatism (Prada et al., 2014; Merino et al., 2019). The interpretation of these bodies as magmatic back-arc oceanic crust is based on their two-layer structure (Grevemeyer et al., 2018; Prada et al., 2020). In the Tyrrhenian, opening subsequently led to mantle exhumation (Prada et al., 2015; 2020), but extension has stopped and the basin is currently being inverted (Zitellini et al., 2020). In the westernmost Mediterranean, the allochthonous terrains are represented by the Alboran Domain that outcrops in southeast Iberia and northwest Africa (Fig. 1a, Garcia-Dueñas et al., 1992), although its offshore extension is poorly constrained. Modern wide-angle seismic data across the eastern Alboran basin supports the existence of magmatic-arc crust (Booth-Rea et al., 2018, Gómez de la Peña et al., 2020) and the interpretation of basement domains across the basin is based on deep-penetration seismic images and integration of seafloor dredging and drilling results (Booth-Rea et al., 2007; Gómez de la Peña et al., 2018).

2.1. The Gibraltar Arc System

The Alboran and the Algero-Balearic basins form the Gibraltar Arc subduction system together with the Betics, the Rif and the Gulf of Cadiz (Fig. 1a). The post-Variscan Mesozoic structuration of the lithospheric domains forming the Gibraltar Arc possibly started in the late Triassic (~230 Ma - Ladinian), when, as a consequence of the first phases of extension between America and Africa, initial extension at the Tethyan Rift occurred. The Tethys ocean between the Iberian and African plates started to open in Early Jurassic times (~190-185 Ma) (Rovere et al., 2004; Martínez-Loriente et al., 2014; Michard et al., 2018). The western part of the Tethys is termed Ligurian-Tethys, and its eastern part is referred as Alpine-Tethys. The western Mediterranean basins, including the Alboran Basin, the Algero-Balearic Basin and the Betic and Rif orogenic belts, formed in the upper plate, above the subducted Ligurian-Tethys oceanic lithosphere and its South Iberian, Adulian and North Maghrebian passive margins (e.g., Lonergan and White, 1997; Booth-Rea et al., 2007; Platt et al., 2013). The subduction process of Alpine-Tethys oceanic lithosphere may have begun in the early Cretaceous (~120 Ma), but it did not affect the Ligurian-Tethys before the Eocene-Oligocene.

2.1.1. The Betic-Rif System

The system comprises the Betic mountain belt in southeastern Iberia and the Rif in north Morocco (Fig. 1a) showing a complex structure that holds evidence of changes in the dominant orientation of the subduction zone. During the Oligocene – Miocene, oblique collision of terrains occurred along the northern and southern branches of the system in the Betics and Rif, whilst in the central segment the Jurassic oceanic lithosphere subducts under the Gulf of Cadiz and Gibraltar arc (Sallarès et al., 2011; 2013). The westward directed thrusting of the Betic-Rif orogenic arc is faced, further westward, by the accretionary prism outcropping in the Gulf of Cadiz (Sartori et al., 1994; Torelli et al., 1997; Gràcia et al., 2003) while towards the East it abuts the Alboran basins that include the fore-arc, volcanic arc and back-arc domains of the subduction system (inset Fig. 1a). The Betic and Rif belts form an arcuate orogenic system that surrounds the marine domain, and consist of a superposition of different tectonics domains. The Betics and Rif mountain belts show equivalent tectonic units, that can be separated into: (i) the foreland basins, (ii) the external zones, (iii) the flysch units, and (iv) the internal zones (inset Fig. 1a) (Sanz De Galdeano, 1990; García-Dueñas et al., 1992; Chalouan and Michard, 2004; Balanyà et al., 2007).

The foreland basins correspond to the Guadalquivir Basin in southern Iberia and the Rharb Basin in northwest Morocco (Fig. 1a). They contain middle Miocene to Pliocene sedimentary sequences (Alonso-Chaves et al., 2004; Chalouan et al., 2009).

The External Zones (Fig. 1a) form a Foreland Thrust Belt (FTB) composed of Mesozoic and Cenozoic sediment overlaying the Iberian and Moroccan continental basements (Sanz De Galdeano, 1990; Crespo-Blanc and Frizon de Lamotte, 2006) (Fig. 1a). The Miocene deformation in this domain is different in Iberia and North Africa. The Betics FTB underwent a thin-skin tectonic evolution, with upper Triassic evaporites commonly acting as a detachment level, while the deeper units of the Rif FTB includes a Paleozoic basement in their nappes reaching greenschist metamorphic conditions typical of thick-skin tectonics (Chalouan and Michard, 2004; Crespo-Blanc and Frizon de Lamotte, 2006; Negro et al., 2007; Jabaloy et al., 2015). The Flysch units (Fig. 1a) contain deformed siliciclastic rocks ranging from the late Jurassic to early Miocene (Burdigalian), deformed during the early to middle Miocene (Luján et al., 2006). They represent pre-tectonic deep-sea sedimentation on the African-Iberian continental margins of the Tethys Ocean, and syntectonic Miocene deposits (Butler et al., 2020). They are structurally sandwiched between the External and Internal Zones (Guerrera et al., 1993; Alonso-Chaves et al., 2004).

The Alboran Domain of the Internal Zones (Fig. 1a), represents the inner part of the orogen resulting from the structural superposition of three allochthonous polymetamorphic terrains. The Alboran Domain terrains have been interpreted as part of the AlKaPeCa terrain dismembered during the opening of the western Mediterranean basins (García-Dueñas et al., 1992; Platt et al., 2005; 2013). Subduction drove terrains to different burial depths, with different degrees of metamorphism and to a gradual collision with the surrounding margins (e.g., Sanz De Galdeano, 1990; Alonso-Chaves et al., 2004). Structurally, from bottom to top, these terrains are the Nevado-Filábride, Alpujárride and Maláguide in the Betics. On the African margin, the Sebtide and Ghomaride units are analogous to the Alpujárride and Maláguide complexes, respectively (Sanz De Galdeano, 1990; Alonso-Chaves et al., 2004; Chalouan and Michard, 2004). The present-day boundaries between these terrains are extensional shear-zones, related to their exhumation (García-Dueñas et al., 1992; Alonso-Chaves et al., 2004; Chalouan and Michard, 2004). The Nevado-Filábride and the Alpujárride/Sebtide complexes exhibit high-pressure low-temperature metamorphism. The metamorphism of the Alpujárride complex has been dated as Eocene, however, this age is still debated, having a clear early Miocene thermal overprint (e.g., Azañón et al., 1997; Sánchez-Rodríguez and Gebauer, 2000; Platt et al., 2003, 2005). The Nevado-Filábride high-pressure metamorphism took place later, between the early to middle Miocene (López Sánchez-Vizcaíno, 2001; Platt et al., 2006; Kirchner et al., 2016). Initially interpreted as an allochthonous complex, the Nevado-Filábride is currently interpreted as autochthonous metamorphosed South Iberian margin basement (Platt et al., 2006; Booth-Rea et al., 2015; Jabaloy-Sánchez et al., 2018). The Alboran Domain forms the basement flooring the West Alboran and Malaga sub-basins (Fig. 1a) (Comas et al., 1999; Gómez de la Peña et al., 2018).

2.1.2. The Alboran and Algero-Balearic basins

The origin, formation process, and evolutionary model of the western Mediterranean basins remains debated. Regions of the Alboran Basin and related (currently emerged) sub-basins were extended during the late Oligocene – Miocene, whereas the Gibraltar Arc and sectors of the Gulf of Cadiz were shortened during the same period (Sanz de Galdeano et al., 1990). Three different hypotheses were proposed to explain the extension leading to the basin formation: (1) post-orogenic extensional collapse related to the convective removal of continental lithospheric mantle (Dewey et al., 1989; Platt and Vissers, 1989); (2)

delamination of lithospheric mantle beneath the orogen (García-Dueñas et al., 1992; Seber et al., 1996; Calvert et al., 2000; Duggen et al., 2003); and (3) subduction of oceanic lithosphere and associated slab rollback (Royden, 1993; Lonergan and White, 1997) and/or slab break-off (Blanco and Spakman, 1993; Zeck, 1999). Improvements in the resolution of the 3D mapping of Mediterranean mantle slabs (Wortel and Spakman, 2000) lend further support to the hypothesis that the Alboran and Algero-Balearic basins were produced by extension kinematically linked to the slab rollback of the subducting plate (e.g., Spakman and Wortel, 2004; Faccenna et al., 2014 and references therein), together with slab-tearing or detachment at the edges of the system (Govers and Wortel, 2005; Mancilla et al., 2015; Hidas et al., 2019). Nevertheless, the 3D geometry, the continental or oceanic nature of the slab, and the spatial and temporal evolution of the subduction system are still debated (e.g., Levander et al., 2014; Chertova et al., 2014a).

The Alboran Basin traditionally has been interpreted as a back-arc basin due to its location with respect to the structural Gibraltar arc, linking the Betics and Rif orogenic belts (Comas et al., 1992; Watts et al., 1993). However, this interpretation considers the basin geographic position in respect to the tectonic arc (Betic-Rif orogen) and not to the volcanic arc, which disagrees with the geodynamic setting of the area. The first evidence of the volcanic arc in the Alboran Basin came from volcanic rock samples (Hoernle et al., 1999; Duggen et al., 2003, 2008) and multichannel seismic reflection images (Booth-Rea et al., 2007). Further mapping of the basement using deep-penetration seismic reflection images and wide-angle seismic profiles supports the existence of three main geodynamic domains in the westernmost Mediterranean: a) a fore-arc basin, represented by the WAB and MB (Gómez de la Peña et al., 2018); b) the magmatic-arc of the central and EAB (Booth-Rea et al., 2007, 2018, Gómez de la Peña et al., 2020); and c) a back-arc basin across the easternmost EAB and the ABB (Booth-Rea et al., 2007; Gómez de la Peña et al., 2018).

During the opening of the Alboran basin, extensional processes were linked to significant magmatic activity, generally in a supra-subduction setting (Hoernle et al., 1999; Maury et al., 2000; Gill et al., 2004; Duggen et al., 2008). Late Oligocene to early Miocene tholeiitic and calcoalkaline dykes, described onshore, intrude the Malaguide and Ronda peridotites complexes (Torres-Roldan et al., 1986; Duggen et al., 2004; Marchesi et al., 2012). This magmatism was followed by a -poorly constrained- middle to late Miocene phase, characterized by calk-alkaline, tholeiitic and shoshonitic volcanism that forms a subduction-related volcanic arc (Hoernle et al., 1999; Duggen et al., 2008; Varas-Reus et al., 2017). Seafloor spreading in the ABB back-arc setting was possibly coeval, as inferred from seismic data (Booth-Rea et al., 2007, 2018; Medaouri et al., 2014; Aïdi et al., 2018). Magmatism waned during the latest Neogene (Messinian) to Quaternary, with limited alkaline volcanism localized mainly on the basin rims and reflecting a source of hot asthenospheric material, rather than subduction related fluids (Duggen et al., 2004, 2008).

The ABB opening kinematics and crustal structure are also debated. Some models suggest a NW-SE opening at ~19 Ma (Rosenbaum et al., 2002; Schettino and Turco, 2011), although most models propose an E-W opening between ~16–8 Ma during the westward migration of the Alboran Domain (Mauffret et al., 2004; Chertova et al., 2014b; van Hinsbergen et al., 2014). Leprêtre et al. (2013) proposed an opening in two stages, an initial opening of the central ABB in a N-S or NW-SE direction, and a second strike-slip stage along the margin linked to westward migration of the Alboran Domain. Recent seismic studies of the crustal structure of the North Algerian margin proposed that a strike-slip margin developed above a STEP (Subduction Transform Edge Propagator, Govers and Wortel, 2005) fault -i.e., above a propagating tear in the underlying slab (Leprêtre et al., 2013; Badji et al., 2015; Hidas et al., 2019).

The crustal structure resulting from the opening process is also debated. Seismic reflection images (Booth-Rea et al., 2007) and coincident wide-angle data (Booth-Rea et al., 2018) support a W to E transition from magmatic-arc crust to back-arc oceanic crust. The S to N change from African continental crust to magmatic-arc crust appears abrupt in seismic images of the Alboran basin (Gómez de la Peña et al., 2018, 2020). Seismic images display a back arc oceanic basement with smooth relief (Booth-Rea et al., 2007), indicating limited tectonic extension during spreading and comparatively more important magmatic processes, which might indicate its formation at intermediate or high spreading rates (Ranero et al. 1997a; 1997b). However, indistinct seafloor spreading magnetic anomalies do not constrain the extent of the oceanic basement domains (Galdeano and Rossignol, 1977) and the spreading rate and age remain undefined. Continuous Moho reflections map the transition from continental or arc crust to back arc oceanic crust (Booth-Rea et al., 2007; Medaouri et al., 2014; Giaconia et al., 2015; Gomez de la Peña et al., 2018). The continuos Moho images support an abrupt transition to oceanic crust, i.e. without mantle exhumation (e.g., Cameselle et al., 2017), in contrast to the nearby Tyrrhenian back arc where abundant mantle exhumation occurs (Prada et al., 2014; 2015).

The Messinian period includes the Mediterranean Salinity Crisis (MSC, ~6–5.3 Ma) (Hsü et al., 1973; Roveri et al., 2014 and references therein). This event has been interpreted as resulting from the closure of the Straits of Gibraltar and the African and Iberian gateways, which produced a rapid sea-level drop, implying subaerial erosion and deep-basin salt deposits (e.g., Rouchy and Caruso, 2006; Rohling et al., 2008; Lofi et al., 2011, García-Castellanos et al., 2020). However, recent studies support that the Straits of Gibraltar was not closed, as the top of the Messinian unit is a paraconformity along much of the WAB. The lack of Messinian erosion in the shallow region of the WAB margins supports that it was not dessicated during the MSC, and that -partial- closure of the Atlantic-Mediterranean corridor occurred at the EAB volcanic arc (Fig. 2, Booth-Rea et al., 2018).

In the latest Miocene, subduction probably stalled (Iribarren et al., 2007; Zitellini et al., 2009). Since late Messinian times, the deformation associated to the NW-SE convergence (4.5–5.6 mm/yr) between the African and Eurasian plates (DeMets et al., 2010; Nocquet, 2012) is deforming the Alboran Basin together with strike-slip and reverse faults (Gràcia et al., 2006, 2011, 2019; Martínez-García et al., 2013; Grevemeyer et al., 2015) that appear to reactivate pre-existing structures (Gómez de la Peña et al., 2018). GPS-derived kinematic vectors indicate that lithospheric-scale structures bound tectonic blocks that move independently (e.g., Palano et al., 2015).

2.1.3. The marine sedimentary record onshore

Several Miocene marine sedimentary sub-basins occur onshore in SE Iberia (Fig. 1b). These depocenters were in continuity with the Alboran and Algero-Balearic basins during the Miocene. These sub-basins formed by extensional tectonics since the late Oligocene until the present-day and are coeval to contractional and transcurrent deformation of the external foreland thrust-belt (García Dueñas et al., 1992; Martínez-Martínez et al., 2002; Giaconia et al., 2014). This extension propagated behind the NW to W migrating the Gibraltar Arc orocline, overstepping previous contractional and transpressive structures (Rodríguez-Fernández et al., 2011; Mancilla et al., 2015). Since the latest Tortonian, these sub-basins -especially in the SE Betics- were tectonically inverted and shortened in a transcurrent setting related to Africa-Iberia plate convergence (Bousquet, 1979; Montenat and Ott d'Estevou, 1990; Ott d'Estevou et al., 1990; Booth-Rea et al., 2004a), and they were uplifted and progressively emerged (Braga et al., 2001; Rodríguez-Fernández et al., 2011).

Uplift and emersion of the onshore Betic depocenters has been ascribed to the interplay between plate convergence and deep mantle mechanisms, like slab tearing and lithospheric-mantle edge delamination under the SE Betics, which produced the important isostatic rebound of the continental margins of the Alboran basin (Duggen et al., 2003, 2008; Garcia-Castellanos et al., 2011; Mancilla et al., 2015). This process is thought to have been propagated westwards during the late Miocene, being recorded by Tortonian evaporites in the Lorca and Fortuna basins on the eastern Betics (Krijgsman et al., 2001) and reaching near the Straits of Gibraltar during the Pliocene (García-Castellanos et al., 2011; Booth-Rea et al., 2018).

The sedimentary infill of the onshore extensional sub-basins recorded a complex tectonic evolution from the late Oligocene to Holocene. This sedimentary evolution is often described as "intramontane" basin evolution within the Betics (Fig. 1b) (e.g., Rodríguez-Fernández et al., 2012). However, the emersion on land of these basins occurred in a late stage of their evolution in relation to (i) their continuous westward displacement in the hanging-wall of regional extensional detachments, and (ii) the development of late Miocene to present contractional antiformal ridges, and associated transcurrent structures among them (Martínez-Martínez et al., 2002; Booth-Rea et al., 2004a; Giaconia et al., 2012, 2013; Azañón et al., 2015). The westward movement of these basins continues nowadays to the west and south-west of the detachment of the Sierra Nevada extensional dome, as attested by GPS measured displacements (Galindo-Zaldivar et al., 2015). This has resulted in significant paleomagnetic rotations of late Miocene sediments within all these "basins" (Cifelli et al., 2006; Crespo-Blanc et al., 2016).

In the basin stratigraphy section, we include a revision of the currently onshore Betic sub-basins, which were connected to the Alboran and Algero-Balearic basins during the late Miocene forming marine gateways to the Atlantic (e.g. García-Dueñas et al., 1992; Rodríguez-Fernández et al., 1999; 2011; Soria et al., 1999; Flecker et al., 2015) (Fig. 1b). The sediments are divided into two groups, corresponding to the older and younger Neogene, a distinction based on the presence or absence of clasts of the subducted basement of southern Iberia (Nevado-Filabride metamorphic complex), exhumed in the core of the Betics (Völk, 1967; Giaconia et al., 2014; Booth-Rea et al., 2015). The Nevado-Filabride complex reached the surface by extensional faults in the Tortonian. These two sediment groups recorded two different extensional exhumation events, early to middle Miocene unroofing of the Alpujarride complex and late Miocene denudation of the deeper Nevado-Filabride complex. These two unroofing events followed after two different crustal thickening phases, the Paleogene for the Alpujarride and early to middle Miocene of the Nevado-Filabride (e.g., Platt et al., 2005, 2006). The older Paleogene-Neogene sediments comprise four sedimentary units deposited between the latest Oligocene and the Serravallian. Meanwhile, the younger Neogene-Quaternary sequence includes Tortonian to Pliocene-Holocene sediments (Fig. 5).

3. Data and methods

To characterize the Alboran and western Algero-Balearic basins, we integrated a new grid of seismic reflection profiles from the Barcelona-CSI (i.e., TOPOMED, EVENT-DEEP, IMPULS and EVENT-SHELF, Fig. 1b) with datasets available from industry (i.e., CAB) and vintage academics (i.e., CONRAD and ESCI, Fig. 1b). The regional distribution of these profiles and their multi-scale resolution allows us to re-evaluate the seismostratigraphy of the entire Alboran Basin. Available dredge information in addition to the academic and commercial wells are also integrated into this analysis in order to calibrate and correlate

the identified seismic units (Fig. 1b). The acquisition characteristics and the processing flow applied to the seismic data sets are shown in Tables 1 and 2.

We used IHS Kingdom Advanced software to interpret the stratigraphy and main structures of the MCS dataset, integrating the multibeam bathymetry map and the well records. We used Generic Mapping Tools (GMT, Wessel and Smith, 1991) to plot the seismic images. The seafloor map analysis and display were carried out using ArcGIS software.

4. Basin stratigraphy

4.1. Seismic units

Recent works mainly focus on the post-Messinian stratigraphy of the Alboran Basin, which is reasonably well established (Martínez-García et al., 2013, 2017; Moreno et al., 2016; Juan et al., 2016). The earlier stratigraphy is well defined in a few regionally restricted studies. In this study, we revised the seismo-stratigraphy for the entire Alboran and western Algero-Balearic basins (Figs. 3, 4), integrating our dataset with previous studies (Jurado and Comas, 1992; Alvarez-Marrón, 1999; Comas et al., 1999; Booth-Rea et al., 2007; Gràcia et al., 2006, 2012; Soto et al., 2010, 2012; Medaouri et al., 2012, 2014; Giaconia et al., 2015; Moreno et al., 2016; Do Couto et al., 2016; Juan et al., 2016). We have unified the stratigraphic nomenclature for all the Alboran and ABB sub-basins (Fig. 3a). The correlation between the units defined in this work (Fig. 3) with previous studies is shown in Figure 4.

We correlate the seismostratigraphic units by their calibrated age. Despite a limited drilling information, particularly for pre-Messinian units in the deep basins, the main unit boundaries are regional unconformities that provide a reliable chronostratigraphy, to correlate units among sub-basins. Following the literature and available drill-sites, and to facilitate comparison with previous works, the units are labelled in three approaches (Fig. 5): 1) Most sediment units are named with Roman numbers from I to VII; 2) Pre-Messinian sediment units of the HBB and PB have no units equivalent to I to VII and are labelled as UT (Upper Tortonian unit), LT (Lower Tortonian Unit) and S-L (Serravallian-Langhian unit); and 3) Due to a restricted distribution, volcanic units overlaying crystalline basement have been labelled starting with a v, and with the first letter of the area where they are found (i.e., A: Alboran Ridge area, Y: Yusuf Fault area, D: Djibouti Plateau area, and C: Carboneras Fault area). When more than one volcanic unit are identified in a given area, increasing numbers indicate older age (i.e., vA1 is the youngest volcanic unit in the Alboran Ridge area).

4.1.1. Sedimentary units

4.1.1.1. Post-Messinian units

Unit I (0-1.80 Ma, Holocene-Pleistocene) shows parallel continuous reflections and ranges between 0.3 and 0.7 s two-way travel time (TWTT) thickness. Near the Alboran Ridge it is subdivided into sub-unit Ia (0-0.78 Ma), characterized by parallel continuous reflections intercalated with chaotic bodies and a maximum thickness of 0.4 s TWTT, and Ib (0.78–1.80 Ma), characterized by high-amplitude, parallel continuous reflections and a thickness ranging between 0.1 and 0.3 s TWTT (Fig. 3a, c, d, Martínez-García et al, 2013).

Unit II (1.80-5.33 Ma, Gelasian-Zanclean) is well stratified and thickens from < 0.5 s TWTT in the EAB to 0.5–1 s TWTT in the WAB (Fig. 3b, e). In the WAB, it can be divided into sub-units U-II (1.80-3.60 Ma) and L-II (3.60-5.33), with L-II showing a comparatively low-reflectivity character (Fig. 3b). Across the Alboran Ridge (SAB and N.AR, Fig. 3c, d), four internal sub-units are differentiated (IIa-d), following the interpretation of Martínez-García et al. (2013). The boundaries of these sub-units are unconformities possibly related to successive deformation pulses in the Alboran Ridge area (Martínez-García et al., 2013).

4.1.1.2. Messinian units

Unit III (6.25-5.33 Ma, Messinian) is made of rather variable deposits. In the deep water EAB and ABB it terminates with the evaporites of the Messinian Salinity Crisis (MSC, 5.96-5.33 Ma). The top of Unit III is often delineated by the "M" reflection, typically an unconformity, but across the WAB and MB it appears as a paraconformity (Fig. 3). In the Alboran Channel and the SAB (Fig. 3c, d) interpreted Unit III may also include the uppermost Tortonian, since it has not been calibrated by drilling. In the HBB-PB and the ABB this unit is well developed and can be divided into sub-unit IIIa (5.96–5.33 Ma) and sub-unit IIIb (6.25-5.96 Ma) (Fig. 3a, f, g). Sub-unit IIIa top layers are irregular sedimentary bodies that look like chaotic mass-transport deposits ("c" in Figures 3a, g), similar to deposits at the same stratigraphic position in neighbouring regions (e.g., Cameselle and Urgeles, 2015). In the easternmost EAB and in the ABB, evaporite deposits form most of the sub-unit IIIa. Where evaporites are found, we correlated sub-unit IIIa with the MSC units defined for the whole Mediterranean region (Fig. 3a, f). These are the *Upper Unit (UU), Mobile Unit (MU)* and *Lower Unit (LU)*, respectively (e.g., Lofi et al., 2011; Giaconia et al., 2014; Roveri et al., 2014). This series are bounded by the Top Surface or Top Erosion Surface (TS/TES), that correlates with the "M" unconformity (Lofi et al., 2011), and the Bottom Surface or Bottom Erosion Surface (BS/BES) (Fig. 3a, f, Lofi et al., 2011).

4.1.1.3. Pre-Messinian units

In the WAB and MB, **Unit IV** (> 6.25 Ma - early Tortonian) is characterized by high-amplitude parallel continuous reflections, almost 1 s TWTT thick (Fig. 3a, b). Ongoing revisions of the Andalucia G-1 well (Fig. 1b) suggests that the upper part of this unit is early Messinian (Sierro, 2018, personal communication). Unit IV is also found at the western EAB (Fig. 3a, e). **Unit V** (early Tortonian–late Serravallian) shows parallel continuous reflections at the top with decreasing reflectivity towards its base, locally reaching >1.5 s TWTT in thickness. **Unit VI** (Serravallian and Langhian) shows spaced, low-amplitude parallel continuous reflections. In the WAB, this unit can be subdivided in sub-units VIa and VIb, being unit VIb characterized by alternate flickering reflections and chaotic layers (Fig. 3a, b). **Unit VII** (possibly of Burdigalian age) is characterized by high-reflectivity discontinuous reflections, underlain by a low-continuity reflection that is interpreted as the basement top.

In the HBB and PB, on the African shelf, three Miocene units are identified: **Unit UT** (late Tortonian) alternating low reflectiviy and well-stratified zones, **Unit LT** (early Tortonian) showing low continuity internal reflections with changing dips, and **Unit S-L** (Serravallian-Langhian) characterized by low-amplitude non-parallel reflections with a poorly defined base (Figs. 3a, g). These units are calibrated with the ages published for the HBB-1 well (Medaouri et al., 2014).

4.1.2. Volcanic units

Volcanic units overlaying the basement occur across a large part of the sub-basins, however their correlation is difficult mainly due to 1) their restricted geographical distribution, 2) uncertainty in age due

to scarce sampling, and 3) the nature of the volcanic processes that tends to produce accumulations near the source. When possible, an age obtained from dredged samples were assigned to the units, and a relative age based on the relationship with other units was proposed. We mapped volcanic units in four distinct areas: The Alboran Ridge (vA units), the Yusuf Fault (vY units), the Djibouti Plateau (vD units) and the Carboneras Fault (vC units). Volcaniclastic units have a clear seismic character (e.g., Fig. 6, 7: vA1 and vA2 units, Fig. 8: Yusuf Ridge and Al-Mansour Seamount, vY1 and vY2 units, Figs. 9, 10: Djibouti Plateau, vD unit; Fig. 11: Chella Bank, vC unit) and sparse dredges confirm their volcanic nature (Aparicio et al., 1991; El Bakkali et al., 1998; Hoernle et al., 1999; Duggen et al., 2004, 2005, 2008) (Fig. 1b). The units may also contain lava flows, although it remains undetermined with seismic images alone.

In the Alboran Ridge area, we identify two units. **Unit vA1**, displays chaotic high-amplitude reflections with low continuity, especially on the upper section. Unit vA1 outcrops at the western part of the Alboran Ridge and dredged rocks recovered from this high confirmed a Tortonian age (9.26-9.37 Ma, e.g., Duggen et al., 2004, 2008) (Fig. 1b). Below, a basal high-amplitude irregular reflection bounds the contact to **Unit vA2** (Fig. 6b CMPs 16000-14000, 7a CMPs 6500-8000). Unit vA2 exhibits chaotic reflections intercalated with low-amplitude and low-continuity reflections (Fig. 7). These volcanic units overlay a basement with high reflectivity (Fig. 3c, d, 6b, 7a), characterized by strong reflections of poor lateral continuity. Tentative correlation with the HBB-1 well supports an age of > 11.63 Ma (pre-Tortonian) for these volcanic units.

The Yusuf Fault area is characterized by three volcanic units (Figs. 3a, e, 8) separated by unconformities. The youngest corresponds to **Unit vY1** that outcrops at the Al-Mansour Ridge (Fig. 1a). Dredged basaltic andesites give an age of 8.7 Ma for the surface layer of this volcanic edifice (Duggen et al., 2004, 2008). High-amplitude reflections intercalate between poor- and well-stratified zones that laterally interfinger with **vY2,** an older volcanic unit. Andesites of vY2 were dredged at Yusuf Ridge (Fig. 1a), yielding a 10.7 Ma age (Duggen et al., 2004, 2008). The vY2 unit is characterized by high-amplitude wavy reflections (e.g., Yusuf Ridge at Fig. 8a). On the eastern flank of the Yusuf Ridge, an older **vY3** unit occurs (Fig. 8c-d). This unit has not been dredged, although due to its seismic character and restricted lateral extension, we infer that it is also of volcanic origin. The base of these units is defined by changes in the character of reflectivity, rather than by a well-defined boundary. The basement below these volcanic units shows an overall low reflectivity (Fig. 3, 8c-d).

Under the sediment units of the Alboran Channel and the Djibouti Plateau, a **vD** volcanic unit displays similar characteristics to the units located in the Alboran Ridge area (Fig. 1a, 3, 9, 10). In the Carboneras Fault area, a volcanic unit, **vC,** is characterized by an irregular top and high-amplitude scattered reflections (Fig. 3, 11b). This unit extends along the northeast Alboran Basin margin towards the Palomares margin. The interfingering among the calibrated sediment units in the area supports a late Tortonian–early Messinian age (Fig. 11b CMPs 12000-17000).

4.1.2. Basement nature and structure

The nature and structure of the basement varies across the Alboran–Algerian basins (e.g., Booth-Rea et al., 2007; 2018; Gómez de la Peña et al., 2018). In this section, we review the available basement data for each sub-basin and their potential implications to interpret the seismic images.

4.1.2.1. West Alboran, Malaga and currently onshore basins

The WAB and MB basins form an arcuate continuous depocenter that mimics the shape of the orogenic front across the Straits of Gibraltar and South Iberia, which often have been described as separate basins. It

contains > 6 s TWTT of sediment (~10–12 km) and it is the thickest and oldest depocenter of the Alboran Basin (Comas and Jurado, 1992; Soto et al., 2010, 2012; Do Couto et al., 2016). The Andalucia G-1, DSDP Site 121, and ODP-161 Site 976 drilling reached metamorphic continental rocks at the basement top (e.g., Comas et al., 1999). This metamorphic basement is the same of the emerged basins on the Betics, and is similar to the Alboran Domain of the the Betics internal domain on land. Volcanism only occurrs along the eastern rim of the WAB and MB basins, as confirmed by dredges from the Algarrobo, Herradura and Ibn-Batouta banks (Fig. 1a; Duggen et al., 2008), as well as seismic images of other volcanic constructions (Gómez de la Peña et al., 2018).

The top of the basement is indistinct and inferred from the base of parallel reflections interpreted as sediments (Figs. 9-17, see Figure 1b for location). At the WAB, the basement top is smooth and deepens from the margins towards the centre of the sub-basin. Along a W-E transect, the basement top is found at ~2 s TWTT at the western margin (Fig. 12a CMPs 20000-16000) and deepens to ~5.5 s TWTT (e.g., Fig. 12a CMPs ~11500) towards the centre of the sub-basin. Similarly, in a NW-SE direction the top of the basement deepens from the NW flank to the depocenter (Fig. 14a), with a maximum sedimentary infill of >7s TWTT (Fig. 14b CMP ~12000), and then shallows again towards the SE flank (Fig. 13a CMPs 15000–11000, 14b CMPs 12000-18000). Figure 15 images the WAB in a SW-NE trending transect. The basement top rises from ~7.5 s TWTT at the depocenter (Fig. 15a CMPs 2000-7000) to ~2.5s TWTT at the sub-basin's flanks (Figs. 15a CMPs 9000–12000). On the rims of the WAB (Fig. 1b), figures 16 and 17 displays the basement at 4.5–6 s TWTT. Towards the east and southeast, volcanic constructions intrude the metamorphic basement (i.e., Ibn-Batouta Bank at Fig. 13b).

Profile TM21 (Fig. 15) images the continuity between the WAB and MB sub-basins, interrupted by the volcanic construction of the Algarrobo Bank (Fig. 15b CMPs 18000–20000). In the MB, profile TM22 (Fig. 11) images the basement at 4–5 s TWTT, masked eastwards by the volcanic buildup of the Chella Bank (Fig. 11b CMPs 12000–16000). The basement at the MB ends abruptly against the Carboneras Fault (Fig. 11b CMPs ~18000), and to the eastwards it is possibly formed by Neogene igneous arc rocks of the "Cabo the Gata" volcanic province (Gómez de la Peña et al., 2018).

4.1.2.2. Habibas and Pytheas basins

Offshore North Africa, the Pytheas and Habibas sub-basins are separated by the Provençaux Bank and each sub-basin delineates a semi-circular low relief in the bathymetry (Fig. 1a). The basement of the HBB was sampled by the HBB-1 well-site, with the recovery of continental metamorphic rocks (Medaouri et al., 2014). In the seismic images, the basement is defined by a general high-reflectivity character, bounded by a poor-defined top reflection (base of Unit S-L) located between ~2 and ~5 s TWTT at the HBB (Fig. 18, 19c) and between ~1 and ~3.5 s TWTT at the PB (Fig. 19b). The basement top defines a syncline (Fig. 18-20).

4.1.2.3. South Alboran Basin

This SW-NE elongated sub-basin, with up to ~1.3 s TWTT sedimentary infill, is located on the African continental platform (Fig. 1a) and runs parallel to the Alboran Ridge. The ODP Leg 161 Site 979 (Fig. 1b) calibrates the shallow sedimentary sequence to the Piacenzian (Fig. 6b, Comas et al., 1999; Juan et al., 2016). Dredged volcanic rocks of the Alboran Ridge basement (Aparicio et al., 1991; Duggen et al., 2004; Gill et al., 2004), together with seismic images, supports that a late Miocene volcanic layer probably extends under the basin (Figs. 6, 7). The base of these volcanic units is inferred corresponding to a marked decrease in the reflection amplitude (i.e., black dots in Figures 6b, c, 7a). These late Miocene volcanics

(Duggen et al., 2004), in some cases covering Tortonian marine marls, also crop out along the southern margin of the basin in the Trois Fourches cape (Fig. 1a, Duggen et al., 2004) and along the southern margin of the basin in the Ras Tarf cape (Fig. 1a, Serravallian basaltic andesites, El Bakkali et al., 1998).

4.1.2.4. East Alboran Basin and the Algero-Balearic Basin

The EAB is a triangular shaped basin (Fig. 1a) limited to the south by the Yusuf Fault system and to the north by the SE Iberian Peninsula, grading to the east into the ABB. Dredges of the Al-Mansour and the Yusuf ridges (Fig. 1) recovered Tortonian volcanic rocks (Duggen et al., 2008). Seismic images show a high-reflectivity package interpreted as a volcanic unit with alternating chaotic and layered reflections, with a base that is delineated by an abrupt decrease in reflectivity (e.g., black dots in Figure 8). The internal geometry of the ridges support that they are volcanic build-ups. The volcanic basement of the EAB continues onshore in the "Cabo de Gata" region (Fig. 1a). These volcanics erupted between the middle and late Miocene (14-6.2 Ma, Turner et al., 1999; Zeck et al., 2000; Duggen et al., 2004). The images show a gradual thinning and change in the crustal reflectivity towards the ABB, interpreted as the transition from volcanic-arc basement of the EAB to back-arc oceanic crust of the ABB (Fig. 21b) (Booth-Rea et al., 2018; Gómez de la Peña et al., 2018; 2020). The ABB is generally inferred to be floored across its deeper region by oceanic crust formed during the middle to late Miocene (Rehault et al., 1984), supported by seismic data (Booth-Rea et al., 2007, 2018; Aïdi et al., 2018).

4.2. Basin analysis and onshore sediment units

4.2.1. Late Oligocene to middle Miocene units

Late Oligocene, Aquitanian and Burdigalian to early Serravallian sediments overlie the Alboran Domain basement (Fig. 22). The Malaguide complex shows a Mesozoic to Cenozoic sediment cover that recorded the tectonic evolution of the Alboran domain (e.g., Lonergan and Johnson, 1998; Martín-Martín and Martín-Algarra, 2002). Here we review the sedimentary units that transgressed over the internal zones of the Betics during the early extensional attenuation of the Alboran domain orogenic wedge. Turbidite systems and deep-basin marls record the progressive denudation of the Betic hinterland between the Chattian to Burdigalian. First, the upper units of the Malaguide complex nappe stack were exhumed, bearing the first Cenozoic apatite fission track ages (44–28 Ma) in Chattian to Aquitanian sediments of the Ciudad de Granada group and Rio Pliego formation (Lonergan and Johnson, 1998; Serrano et al., 2006). The first metamorphic minerals appear locally around 19 Ma, including clasts of continental lithospheric-mantle peridotites in the early Burdigalian Viñuela group (e.g., Aguado et al., 1990; Lonergan and Mangerajetzky, 1994; Serrano et al., 2007). Their presence records the exhumation of deeper metamorphic units forming the Alpujarride complex (Lonergan and Johnson, 1998). It is composed of a shallowing upward sequence of pelagic sediment, frequently including volcano-sedimentary chert intercalations (Fig. 5). These sediments are described in numerous of the so called "intramontane basins" of the Betics, such as the Lorca, Vera, Granada and Malaga basins, among others (Fig. 22) (Bourgois et al., 1972; Boullin et al., 1973; Aguado et al., 1990; Rodríguez-Fernández and Sanz de Galdeano, 1992).

The early to middle Miocene sequence is present in the Central and Eastern Betics with two additional units (Fig. 5). A late Burdigalian to Langhian sequence contains from bottom to top, red conglomerates, sandstones with echinoderms and lamellibranchia, platform limestones, turbiditic marls and continental conglomerates (Barragán, 1997; Giaconia et al., 2014). An upper unit is made of Serravallian open-marine turbidites, capped by an early Tortonian continental sequence of red conglomerates and lacustrine silty sandstones with gypsum. This sequence, or parts of it, has been described in sediment depocenters onshore

in the eastern and central Betics, such as Lorca, Vera, Granada, and Guadix-Baza (Figs. 1b, 22) (Rodríguez-Fernández and Sanz de Galdeano, 1992; Braga et al., 1996; Booth-Rea et al., 2004b; Giaconia et al., 2014). In these basins, middle Miocene sediments are syntectonic in relation to north-south directed extensional detachments described in the central and eastern Betics (García-Dueñas et al., 1992; Crespo-Blanc et al., 1994, 1995; Booth-Rea et al., 2005).

Offshore, the oldest sediment drilled or extruded through mud volcanoes, are dated as Aquitanian – Burdigalian. Although, these sediments include older Mesozoic and Tertiary sediment clasts inferred to be part of an olisthostromic unit (Comas et al., 1999; Sautkin et al., 2003). Only the **WAB-MB** and **HBB-PB** sub-basins record the early Miocene sedimentation. The oldest is Unit VII, only identified at the WAB and MB (Fig. 1a), largely affected by intense shale mobilization. The areas free of mud diapirism are characterized by discontinuous reflections that onlap the basement (Fig. 13a CMPs 20000–15000, 15a). Maximum thickness is ≤ ~3 s TWTT (Fig. 15a CMPs 2000-6000), and thins to ~1 s TWTT into the MB (Fig. 11a). Unit VI onlaps unit VII (Fig. 15a CMPs 7000–9000). Sub unit VIb displays either a chaotic reflection configuration (Fig. 13a CMPs 20000–16000) or sub-parallel, laterally continuous, reflections (Figs. 14b CMPs 10000–14000, 15a, 17). Units VIb and VII have been traditionally associated to "overpressured units" (Comas et al., 1999; Soto et al., 2012; Lopez-Rodríguez et al., 2019), source of mud diapirism in the WAB (e.g., Figs. 12a CMPs 14000–12000, 14a-b CMPs 4000–10000). Some diapirs pierce the sediment cover to the seafloor, generating mud volcanoes (Fig. 15a CMPs 6000–7000, 17 CMPs 3000–2000). Cores from mud diapirs contain Paleogene and Mesozoic sediment clasts within an early Miocene matrix (Sautkin et al., 2003). In the HBB-PB, well HBB-1 recovered Langhian to early Serravallian sediment (Unit S-L) above basement (Medaouri et al., 2014). Here, the basement high-reflectivity is locally laterally continuous (Fig. 15, 19).

4.2.2. Late Miocene units: late Serravallian, Tortonian and Messinian

During the late Serravallian, Tortonian and Messinian, sedimentation continued at the **WAB-MB, HBB-PB** and the now emerged **Betics** basins. Magmatic activity in the **SAB**, Djibouti Plateau and **EAB** began at this stage, which was coeval to extension (Fig. 1a).

In the **eastern Betics**, two sedimentary units were deposited during the Tortonian (Fig. 5, 22). The lower unit comprises (from bottom to top) conglomerates, calcareous sandstones and marls, deposited in transitional marine environments, capped by red continental conglomerates with Nevado-Filábride boulders between 11.6 and 9 Ma. This unit represents syn-rift deposits (Booth-Rea et al., 2004b, Giaconia et al., 2014), which continues through the overlying late Tortonian unit (9-8 Ma). This later unit is formed, from bottom to top, by deltaic conglomerates, sandstones and siltstones of transitional and marine facies, deepening into turbiditic marls and limestones with sand and silt intercalations of the Chozas Formation (Fig. 5, Ruegg, 1964). The late Tortonian is the period with greatest tectonic subsidence across Alboran and the currently onshore Betic marine basins (Rodríguez-Fernández et al., 1999). However, in the south-easternmost Betics, marine restriction initiated at this stage with the development of widespread alluvial fans and deltaic systems that are laterally interfingered with the Chozas marls (~8 Ma), and were closely followed by evaporitic deposition at 7.8 Ma in the Lorca and Fortuna basins (Krijgsman et al., 2001). In some cases, dacite volcanics are intercalated with the Chozas marls. Most of the shoshonitic Si-K rich volcanism in the Eastern Betics was coeval to the extension and the deposit of the Chozas unit (Duggen et al., 2003, 2004). The two Tortonian sedimentary units deposited during extensional tectonics in semigrabens overlying westward-directed detachment faults. These detachments exhumed the deepest metamorphic units of the Betics (Nevado-Filábride complex) along the axis of elongated core complexes,

probably under a general transtensive regime (Johnson et al., 1997; Martínez-Martínez et al., 2002; Giaconia et al., 2014; Hidas et al., 2016). The Sierra Nevada core-complex detachment has approximately 100 km of hanging-wall displacement (Martínez-Martínez et al., 2002), occurring between 13-3 Ma according to apatite and zircon fission-track ages in the footwall to the extensional detachment (Johnson et al., 1997; Vázquez et al., 2011). Thus, large displacements are expected for the Tortonian basins in the hanging-wall of the extensional system, which should be taken into consideration in paleogeographic reconstructions of the region.

A progressive angular and laterally erosive unconformity bounds the base of the latest Tortonian to Messinian sedimentary unit (Fig. 5, 22). This unit includes the fully marine Turre formation (Völk, 1966), the evaporitic Yesares Formation (5.96–5.6 Ma), and the Lago-mare Feos formation (5.6–5.3 Ma) (Krijgsman et al., 2001). The Turre Formation shows a transgressive sequence that includes the Azagador temperate carbonates calcirudite member (8–7.24 Ma) later deepening into the Abad marls (7.24–5.96 Ma) (Krijgsman et al., 2001; Martín et al., 2003). Shoshonitic volcanics also occur intercalated in the Azagador member, drilled in the Vera basin (Booth-Rea et al., 2003).

The angular erosive unconformity at the top Tortonian is associated to a basin contractive inversion related to NW-SE convergence between Africa and Iberia (Ott d´Estevou and Montenat, 1990; Booth-Rea et al., 2004a). During the late Tortonian-Messinian sedimentary cycle, between 7.8 and 7.37 Ma, several Betic depocenters initiate their isolation from open-marine conditions with the deposition of evaporites in the Granada, Lorca and Fortuna basins (e.g., Krijgsman et al., 2001; Corbi et al., 2012). In the Lorca and Fortuna basins, the latemost Tortonian evaporates and coeval continental sediments seal most of the late Miocene rifting phase (Booth-Rea et al., 2007).

In the **WAB-MB** depocenter, Unit V (late Serravallian–early Tortonian) and Unit IV (late Tortonian to Messinian) (Fig. 3) represent this period. Unit V thins from ~2.7 s TWTT in the WAB (Fig. 13a) to <1 s TWTT in the MB (Fig. 11a). In the WAB, Unit V thickens towards the centre of the basin, and onlaps older units and basement rocks (Fig. 13a CMPs 20000–15000). Unit IV thickens from 0.9 s TWTT at the WAB to ~1.3 s TWTT at the MB (Fig. 11a), and onlaps Unit V (Fig. 13a CMPs 20000–18000). Unit III (late Messinian) has the most variable character across the entire Alboran Basin. The top of this unit is a para-conformity across most of the WAB and MB (Figs. 2, 11a CMPs 5000-10000, 12, 17), being erosive only at the deeper part of the basin, particularly in the latitude of the Straits of Gibraltar and also near the basement highs and diapiric structures (Figs. 2, 13 CMPs 17000-15000, 14b CMPs 500-3000 and 13000–15000). In the deepest sector of the WAB, Unit III is formed by deposits with chaotic appearance topped by an erosional surface (Figs. 13a CMPs 17000-15000, 11 CMPs 500-4000). In the eastern sector of the MB, sediments are intercalated with volcanics (vC) extending from the Chella Bank, which displays prominent aprons on either side (Fig. 11b CMPs 11500–17000). The volcanic apron onlaps Unit V and underlies Unit IV and younger sediments, supporting a Tortonian age for the volcanism. Further south, the same occurrs for the volcanic unit of the Djibouti Plateau (vD) (Fig. 1a, 9, 10), which onlaps Unit V and is covered by Unit IV implying a Tortonian age (Fig. 9 CMPs 4000–2000). Profile ESCI-Alb1 (Fig. 9) runs across the MB and the Djibouti Plateau showing the onlap of sediment Unit III, (perhaps Units III and IV, as the age at the base of the sedimentary sequence is unknown), further supporting a late Tortonian age for the vD units (Fig. 10).

In the **HBB-PB**, Unit LT (Lower Tortonian) shows low-continuity reflections with changing dips and variations in thickness, (0.1–1 s TWTT, Figs. 18-20) possibly indicating folding that appears to be syn-sedimentary (Fig. 19d). Units S-L and LT define a gentle syncline thickest at the basin depocenter of the

HBB (Figs. 18, 19c) and PB (Fig. 20) filled by the late Tortonian Unit UT which onlaps the previous folded units LT and L-S (Figs. 18, 19c-d). Unit UT is overlapped by Unit III (Figs. 18, 19c). The upper part of Unit III are chaotic discontinuous deposits (c at Fig. 18, 19c). The M reflection presents a marked erosive character at the HBB (Figs. 18, 19b CMPS 3000–4000, 19c CMPs 11000–10000) and some sectors of the PB (Fig. 20b 19000-17500), while it appears roughly concordant in other sectors of the PB (Fig. 20a CMPS 13000-11000). Contrasting with units LT and UT, the Unit III strongly thickens towards the depocenters of the HBB and PB (Figs. 18, 19, 20).

In the **SAB,** stratigraphy supports the hypothesis that the first volcanic activity began in late Serravallian–early Tortonian times. Two volcanic units are identified: Unit vA2 with a top and a base defined by gradual changes in reflectivity (i.e., black dots in Fig. 6b, c). Unit vA1's (Fig. 6b) internal configuration consists of alternating high-amplitude reflections and chaotic zones (Fig. 6b CMPs 17000–17500) with sub-parallel reflections (Fig. 6b CMPs 16000–14000), similar in character to other volcanic units. Unit III is the first non-volcanic sediment in this area, possibly of late Tortonian to Messinian age, locally identified and filling volcanic-basement lows (e.g., Fig. 6c CMPs 12000–10000 and CMPs 7000–6000). The top of Unit III, the Messinian M reflection, directly overlies volcanic basement highs (Fig. 6c CMPs ~10000) and appears conformable in the deeper sectors of the SAB (Fig. 6c CMPs 7000-6000). Unit III is < 0.5 s TWTT, thickening towards the Alboran Ridge to ~1.2 s TWTT (Fig. 7c).

The volcanic basement of the **EAB** was generated at late Serravallian – early Tortonian times. Ages of dredged rocks (e.g., Duggen et al., 2004) and seismic images indicate three successive volcanic episodes in this area. In the transition to the ABB, vY3 is identified (Fig. 8c, d). In the west, unit vY2 occurs next to the Yusuf Ridge (Fig. 8a CMPs 12000–11000). Unit vY1 crops out at the Al-Mansour Ridge (Fig. 8a CMPs 11250–13500). The limit between units vY2 and vY1 is not sharp, and they may overlap in time, inter-fingering with lateral changes of facies (Figs. 8a CMPs 9500 - 11500, 8b CMPs 4000–1000). Unit IV locally overlies the volcanic basement of the eastern EAB (Fig. 8a) with a toplap geometry against the base of Unit III (Fig. 8a CMPs 9250–9750). Unit IV terminates towards the ABB, where Unit III overlies the volcanic basement and thickens to ≤ 1.2 s TWTT. The top of Unit III ("M" reflection) is erosive at the western sector (Fig. 8a), and concordant in the east as the basin deepens (Figs. 8a-d). Clear evaporate deposits occur only at the easternmost EAB and the ABB (Figs. 8c, 8d, 21).

4.2.3. Plio-Pleistocene units

After the MSC, marine sedimentation in the basins now outcropping in the **Betics** only continued in the south-easternmost depocenters, like the Vera, Sorbas and Níjar basins, together with some coastal regions near the Malaga sub-basin (Braga et al., 2003; Guerra-Merchán et al., 2010; do Couto et al., 2014). Continental deposition continued in several onshore basins, such as the Guadix-Baza and Granada basins (Fig. 1b), coeval to further extensional faulting in the central Betics that continues nowadays (Fig. 22, e.g., Azañón et al., 2004; Martínez-Martínez et al., 2006; Galindo-Zaldívar et al., 2015). **Offshore**, Plio-Pleistocene units are correlated across the entire basin, as they are not confined to the sub-basins depocenters. Instead, these units onlap the basement highs, covering the entire region. Different units denote local tectonic features.

Unit II (Zanclean–Gelasian) is associated to contourite and turbidite deposits (Estrada et al., 1997; Palomino et al., 2011; Somoza et al., 2012). In the SAB, it is affected by the Alboran Ridge deformation, and four sub-units are identified (Sub-units IIa-d, Martínez-García et al., 2013). Sub-units IId and IIc are characterized by parallel reflections, and they onlap the Messinian Unit III, as well as the volcanic basement. Their thicknesses (0.35–0.4 s TWTT) are fairly constant, except in the easternmost SAB (Fig.

7c), where they thin away from the Alboran Ridge. Sub-unit IIb shows a similar seismic expression as Unit IIc. Sub-unit IIb thickens by ~0.5 s TWTT towards the depocenter (Fig. 7c) and its top corresponds to an erosional unconformity (e.g., Fig. 7b CMPs 5000–4000). The boundary between sub-units IIa and IIb is interpreted as a hiatus from 2.52 to 2.45 Ma, based on the correlation with ODP-161 "Site 976" (Martínez-García et al., 2013). Sub-unit IIa onlaps Unit IIb and has also an erosional top (Fig. 7b CMPs 5000–4000, Fig. 7c CMPs 5250–7000). These two bounding unconformities are identified in the southern sector of the WAB, and possibly extend into the western sector of the EAB. In the eastern EAB and the ABB, Unit II shows parallel undisturbed reflections (Fig. 8).

Unit I (Calabrian–Upper Pleistocene) exhibits similar characteristics across the WAB, MB, HBB, EAB and ABB (e.g., Figs. 8, 11, 15, 18). In the WAB and the HBB, Unit I gently thickens towards the basin depocenter (Fig. 15a, 19b). In the SAB, it is divided into sub-units Ia and Ib, separated by an angular unconformity related to the Alboran Ridge tectonics, with sub-unit Ia onlapping Ib (Fig. 7a CMPs 7000–8000).

5. Interpretation and discussion

5.1. Formation and evolution of the West Alboran and Malaga sub-basins

The first basin infill correspond to Unit VII, which has been drilled offshore and dated as Aquitanian - Burdigalian. Onshore, the denudation of the upper units of the Alboran domain is recorded in the Oligocene-Aquitanian sediments of the Ciudad Granada group, which has been especially well studied at the Rio Pliego formation in the Eastern Betics (Lonergan and Mangerajetzky, 1994; Lonergan and Johnson, 1998; Serrano et al., 2006). Unit VII is interpreted as an olistostrome (Comas et al., 1999; Martínez del Olmo and Comas, 2008; Soto et al., 2012), or as part of the Malaguide complex (do Couto et al., 2016). However, Unit VII internal geometry and thickness appear fairly regular in some sectors, although extensive mud diapirism at the WAB makes its regional-scale depositional geometry unclear in seismic images, supporting a post-depositional deformation by overpressure-related remobilization processes. Units VIa and V slightly thicken towards the depocenter (e.g., Fig. 15a CMPs 2000–9000). This thickening is more pronounced in Unit IV, with fan-shaped strata towards the center of the basin (e.g., Fig. 15a CMPs 2000–9000). This unit is topped by the M reflection. Sedimentary infill is > 7 s TWTT in the WAB (Figs. 14b, 15a) and 4 s TWTT in the MB (Fig. 11), indicating that subsidence varied between sub-basins. This variation in subsidence is likely related to changes in basement thickness (Gómez de la Peña et al., 2018).

The top of Unit III is concordant in most of the MB and WAB (Figs. 2, 11a CMPs 5000–9000, 14b CMPs 10000–14000, 15a CMPs 2000–7000, 17). It only shows an erosive character near the basement highs, at the western basin flanks near the Straits of Gibraltar (Figs. 2, 13a CMPs 17000–15000, 15a CMPs 8000–9500), and at the deepest water sector of the sub-basin (Figs. 2, 11 CMPs 500-5000; Booth-Rea et al., 2018). This lack of erosion at shallow sectors supports that the WAB and MB were not affected by a MSC sea level drop (Booth-Rea et al., 2018). The erosional channels observed in the deepest-water sector of the Messinian sub-basin may have formed under submarine conditions, related to deep countouritic currents of latest Messinian or Zanclean age. This is supported by the presence of similar, younger comparatively large intra-Pliocene erosive channels in the region, as well as the present-day erosive features at the sea-bottom of the Straits of Gibraltar (Booth-Rea et al, 2018). In the WAB, Unit III has traditionally been interpreted as a thin package with discontinuous and chaotic internal structure (e.g., Comas et al., 1999;

Figs. 9-17), which may be the equivalent of the latest Messinian chaotic deposits found at the HBB (Figs. 18, 19) and in the nearby Valencia Trough (Cameselle and Urgeles, 2015). Due to the absence of an erosional unconformity at the top of the Messinian unit in most sectors of the WAB and MB (Fig. 2, Booth Rea et al., 2018, and this work), and assuming a similarity in the seismic expression of the Messinian sequences at the HBB-PB and the WAB-MB, we propose a different interpretation of the units in the WAB (Fig. 23). The new interpretation implies a thicker Unit III (Fig. 23d-e), which is in good agreement with the thickness of Unit III in other depocenters (Fig. 23). The thickness of Unit III in the WAB-MB has not been constrained by drilling, and the proposed interpretation might be further tested with the revision of the ages of the early Pliocene and late Miocene sediments drilled in the Andalucia G-1, ODP-161 Site 976 and DSDP 121 wells.

Pliocene units cover the entire Alboran basin, presenting similar seismic characteristics along and across the basin. These observations imply three temporally and spatially different phases of subsidence for the WAB and MB: 1) Pre-Burdigalian, 2) Serravallian-Messinian, and 3) Pliocene-Holocene. The first pulse should have been previous to the deposition of Units VII and VI because they are infilling the basement lows and show little evidence of syn-sedimentary extension. Assuming that the unit thickness is fundamentally driven by subsidence, and provided that there is enough sediment supply as appears likely in this context, the second pulse initiates with Unit V and accelerated during the deposition of Unit IV (Tortonian), with fan shape stratal geometry towards the WAB center. Subsidence changed during the Pliocene-Holocene, as sedimentation is no longer confined to individual depocenters delineating the sub-basins, and extends over most basement highs across the whole region with similar depositional characteristics. There is an apparent lack of extensional structures that could control the sub-basins extension and subsidence, although basement faults may be masked by magmatic activity across the eastern Alboran. Thus, much of the region displays an enigmatic long-term subsidence that will be further discussed in section 7.

5.2Formation and evolution of the Habibas and Pytheas sub-basins

The HBB-PB contains a sequence of Langhian-Tortonian sediment units that are folded. The folded stratal geometry of unit S-L supports syn-sedimentary Serravallian–Langhian deformation (Figs. 18 CMP 6000-2000, 19c). The overlaying unit LT (early Tortonian) also exhibits folding with steeply-dipping reflections that onlap unit S-L (Fig. 18 CMPs 6000–5500). In Unit LT, top and base are roughly parallel, delineating a deposit of approximately constant thickness. Unit UT (late Tortonian) is comparatively less deformed, onlaps unit LT and changes in thickness delimite its lateral extension (Figs. 18 CMPs 6000–1000, 19c CMPs 10000–11000). Deformation appears limited to pre-Messinian units. Post-Tortonian sediment shows parallel reflections onlapping unit UT (Figs. 18-20). The sedimentary package thins abruptly towards the sub-circular basin flanks (Fig. 1a)—with the depocenter located at the centre of the basin.

We propose that units S-L and LT (Langhian–early Tortonian) are syntectonic, with tilting gradually attenuated during deposition of late Tortonian Unit UT. The end of local subsidence and the folding pulse agree with the end of an extension phase proposed by Medaouri et al. (2014) for the Algerian platform, based on industry seismic lines and well data. The basin geometry is peculiar because it appears with a similar concave geometry along perpendicular transects, without clear normal faults bounding the sediment accumulation. We interpret this geometry as a pull-apart basin, mainly originated by subsidence in a transtensional setting. Deposition of Unit III occurred in a different tectonic setting, dominated by gentle basin-wide subsidence, leading towards the present-day configuration.

5.3. Formation and evolution of the South Alboran sub-basin

The SAB volcanic basement is Tortonian, and the oldest non-volcanic sediment is late Tortonian(?)-Messinian in age. The later evolution is influenced by tectonics causing the uplift of the Alboran Ridge. In agreement with Martínez-García et al. (2013), we identify three main contractional pulses. These pulses produced distinct contractional structures, tighter in the Eastern and Central Alboran Ridge, and broader towards the west, which indicates a decreasing deformation from East to West.

Different to previous works (e.g., Comas et al., 1999), we interpret the Messinian Unit III as pre-tectonic to the contractional phase. The M reflection marks the top of Unit III, which corresponds to an erosional unconformity across much of the sub-basin and is generally well-defined. Unit III displays internal parallel reflections with concordant contacts (Fig. 7c CMPs 5250-6000). Thus, we interpret Unit III deposition as previous to any major contractional pulse related to the uplift of the Alboran Ridge. While Unit III internal strata delineate constant thickness layers in the core of the main fold, Unit II thins towards the shallowest part of the AR, indicating a syn-tectonic deposit (Fig. 7).

Three intra-Pliocene discontinuities provide an accurate chronology of the deformation, also studied by Martinez-Garcia et al. (2013). The oldest Pliocene units IId and IIc onlap the M unconformity. These units show gentle variations in thickness, like the wedge-shape geometry of Unit IIc (Fig. 7a CMPs 6250–8000). In agreement with Martínez-García et al. (2013), we interpreted that the first compressive pulse occurred in the early Pliocene, during the deposition of units IId and IIc. Unit IIb thins towards the Alboran Ridge (Fig. 7c CMPs 5250-8000), and may represent a second deformation pulse during late Pliocene to earliest Pleistocene times (3.28–2.45 Ma). Unit IIa fills depressions, onlapping Unit IIb. Unit Ib base is erosive partially truncating Units IIa and IIb, locally cutting to units IIc and IId (Fig. 7b CMPs 6000–5000). Unit Ib onlaps its erosive base thinning lateraly, confined within uplifting and contractional structures. Unit Ia shows a similar discordant character, thinning towards the Alboran Ridge. The unit's geometry indicates a tectonic slow-down period when the erosion of Unit II occurred, between the Piacenzian contraction and the deposit of Pleistocene Unit Ib. The wedge shape configuration and thinning towards the Alboran Ridge of Unit I imply a third tectonic pulse during the early Quaternary (Martínez-García et al., 2013). The faulting affects the shallowest units and the seafloor (Figs. 7b CMPs 6000–5000, 7c CMPs 6750–6250), supporting that the Alboran Ridge is actively uplifting at the present.

5.4. Formation and evolution of the East Alboran and the Algero-Balearic basins

The EAB and the ABB basement contains at least three volcanic units, identified in the seismic images as vY1, vY2 and vY3. In the westernmost area (Fig. 8a), the uppermost part of sediment Unit IV has been interpreted. The thickness of Unit III significantly increases from west to east, with maximum values further east in the ABB (Figs. 8d CMPs 4000-1500), where it is characterized by the presence of evaporites (Figs. 8c CMPs 9500–13000, 8d CMPs 4000–1500, 21b CMPs 9000–12250).

In the east EAB and west ABB, the evaporite layer (MU) is deformed by halokinesis, despite a thickness of <0.3 s in TWTT. Profiles TM13 (Fig. 8c) and TM23 (Fig. 21b) reveal gliding structures, with sediment above the MU sliding downslope, where the MU base acts as a weak décollement level. This gliding generates listric faulting up slope (Figs. 8c CMPs 9250–10000, 21b CMPs 9000–10500). Based on the wedge-shaped geometry of Unit I infilling the accommodation space generated by faulting and the rather constant thickness of Unit II, halokinetic processes began at the initial deposit of Unit I (~1.8 Ma), continuing at the present, as faulting affects the seafloor (Gómez de la Peña et al., 2016). Unit II changes from four sub-units in the west (Fig. 8a CMPs 9500-11500) associated to the Alboran Ridge deformation (Martinez-Garcia et al., 2013), to one unit in the east (Fig. 8d).

The geometrical relation between sediment units and the age of the volcanic units, supports that the Al-Mansour Seamount relief is a volcanic construction, while the Yusuf Ridge, which is bounded by the Yusuf Fault on its southern flank, may have resulted from a combination of volcanic and tectonic processes. The Al-Mansour Seamount depicts a triangular shape in cross section (Fig. 8a CMPs 11000–14000), which together with the geometry of the volcanic units support a volcanic construction. The top of this high has been dated at 8.7 Ma (vY1 unit), older than the deposit of the sediment infill. Sediment Units I-III onlap the flanks of Al-Mansour, showing little deformation and supporting that volcanism was active prior to the first deposit of Unit III. The Yusuf Ridge is also a volcanic high. Units II and I onlap the Yusuf Ridge flanks (Figs. 8a CMPs 8000–10000, 8b CMPs 6500–5000), and Unit II slightly thins towards the Yusuf Ridge, while Unit I abruptly thins above it. This geometry indicates syn-sedimentary activity during the deposition of Unit II that increases during the deposition of Unit I. Thus, the Yusuf Ridge relief is possibly build up by Tortonian or older volcanic activity (vY2, ≤ 10.7 Ma old (Duggen et al., 2004)), and post-Messinian tectonic compression.

6. Implications for West Mediterranean geodynamics models

Three groups of geodynamic models calling for different lithospheric processestry to explain the formation of the westernmost Mediterranean region:

i. *Convective removal* of orogenic Betics-R f thickened lithospheric mantle due to gravitational instabilities (Dewey, 1988; Platt and Vissers, 198[illegible] Platt et al., 2003).

ii. *Mantle delamination after continental subduction* of thickened continental lithosphere, leading to asymmetric removal envisaged as the peeling back of subcontinental lithospheric mantle (García-Dueñas et al., 1992; Seber et al., 1996; Calvert et al., 2000).

iii. *Subduction models* inferring oceanic slab rollback (Royden, 1993; Lonergan and White, 1997), slab break-off, or a sequence of both (e.g., Zeck, 1999). All models propose extension above the slab with variations related to slab geometry, and/or changes in convergence rate. Slab break-off models propose upper-plate extension caused by the replacement of the cold slab by hot asthenosphere (Blanco and Spakman, 1993).

Upper mantle tomography has given support for subduction-based models (Wortel and Spakman, 2000; Bezada et al., 2013). Growing evidence supports an E-W directed shortening on land -i.e., terrain displacement with respect to the foreland (Platt et al., 2013; Gonzalez-Castillo et al., 2015)- and similar coeval to younger marine and land extension direction (García-Dueñas et al., 1992; Bouyahiaoui et al., 2015; Garate et al., 2015). This E-W shortening direction contradicts the proposals of radial extension that pure orogenic lithospheric models supported (Dewey, 1988; Seber et al., 1996; Platt and Vissers, 1989; Calvert et al., 2000). However, a gravitational spreading component driving the extension may have occurred in a slab rollback context, whereas the NW-SE plate convergence may have distorted the pattern of extension. Geochemistry of magmatic-arc rocks can be better explained by a time sequence of subduction-related melts (e.g., Duggen et al., 2008). Current tomographic upper mantle models support that slab rollback may have been followed by lithospheric tearing under the Betics (Fig. 24, Bezada et al., 2013; Chertova et al., 2014b; Fichtner and Villaseñor, 2015). However, it has not yet been possible to unequivocally differentiate the continental or oceanic nature of the slabs (Levander et al., 2014). The type

of slabs needs to be resolved, and their kinematic evolution integrated with surface geology to explain the evolution of the arcs and basins (e.g., Garcia-Castellanos and Villaseñor, 2011; Spakman et al., 2018).

6.1. Available observations

A geodynamic model should explain the evolution of the sediment infill, the structure and nature of the basement, the slab distribution, and the tectonic history of the basins. Available observations to be integrated include:

6.1.1. Slab dimensions and geometry

Recent Full Waveform Inversion models refined the image of slabs in the mantle (Fichtner and Villaseñor, 2015). A slab extends from under the south of the Straits of Gibraltar until the eastern Betics, being detached eastward of the western Betics (near Malaga), where it is first imaged at ~200 km depth. Below northern Morocco there is no velocity anomaly indicating a slab (Fig. 24 b-c). Receiver functions across the Betics have been interpreted to show that the slab is the Iberian lithosphere overthrusts by the Alboran Domain (Mancilla et al., 2015).

6.1.2. Magmatic activity

Geochemical analyses of volcanic rocks revealed three main groups: the oldest group, with tholeiitic and calk-alkaline affinity, sampled at the center and near the margins of the Alboran Basin, the second group of Si-K rich shoshonitic magmatism onshore in the Eastern Betics and Rif, and the youngest group exhibiting alkaline affinity and mainly located on land (Duggen et al., 2008; Lustrino et al., 2011; Carminati et al., 2012) (Fig. 24 a). The tholeiitic and calk-alkaline rocks are associated with subduction-related fluids, the shoshonitic Si-K rich magmatism indicates partial melting of the subcontinental crust in a suprasubduction setting, while the alkaline Si-depleted volcanism appears related to the asthenospheric mantle upwelling, interpreted to replace delaminated or teared lithosphere (Duggen et al., 2005; Varas-Reus et al., 2017; Hidas et al., 2016, 2019).

6.1.3. Crustal structure

Basement samples together with deep MCS images support four main types of crust under the westernmost Mediterranean: (i) < 10 km continental crust under most of the WAB and MB, (ii) ~20-30 km thick continental crust under the north African Margin, (iii) ~8-16 km thick magmatic-arc crust under the EAB and SE Iberian margin, and (iv) 6-7 km thick back-arc oceanic crust under the ABB basin (Booth-Rea et al., 2007, 2018; Giaconia et al., 2015; Gómez de la Peña et al., 2018) (Fig. 24 a).

The Moho depth obtained from earthquake data with onshore recordings does not image well the thickness variations under the offshore basins (Mancilla and Diaz, 2015; Díaz et al., 2016), but provides a good estimation for surrounding onshore areas. Moho depth ranges from ~55 km under the Gibraltar Arc to ~40 km west of Al-Idrissi, Trougout and Nekor Fault systems (Fig. 1, 25a) (Díaz et al., 2016), abruptly changing to the east to 25–35 km (Fig. 24 a; Mancilla and Diaz, 2015; Díaz et al., 2016). Along the NE Moroccan margin and in NW Algeria, the presence of IP-LT metamorphic rocks in the Temsamane units (eastern Rif) suggests transpression in an oblique collisional setting before the Tortonian (Rupelian-early Serravallian, ~33–13 Ma, Negro et al., 2008; Booth-Rea et al., 2012; Jabaloy-Sánchez et al., 2015; Azdimousa et al., 2018), followed by extension (late Serravallian-Tortonian, ~12–7 Ma, Booth-Rea et al., 2012). The proposed age for the transtensional processes in the Temsamane units are broadly consistent with the extensional processes observed at the HBB and PB offshore basins.

6.1.4. Basin evolution

The evolution of the marine sub-basins has several characteristics that place constraints on the geodynamic models:

- The oldest two depocenters developed above distinct continental domains and evolved differently. The WAB-MB developed on the Alboran Domain continental crust and migrated westward together with the overriding Alboran Domain plate; while the HBB-PB developed on the North African continental margin that has remained attached to Africa.

- The arcuate WAB-MB, interpreted as the fore-arc basin (Gómez de la Peña et al., 2018), contains the oldest little derformed sediment infill, so that the geometry of the contemporary subduction front should be consistent with the WAB-MB depocenters.

- Migration of the WAB-MB is interpreted to be associated to slab rollback. However, since Messinian times, magmatism and extensional processes in the arc and back-arc waned, so at early Pliocene times, slab rollback must have strongly slowed down or stop and the WAB-MB was close to its present position.

6.1.5. Timing of extension and Pliocene contractional reorganization

The initiation of the oldest, western sub-basins of the Alboran Basin is not well established, possibly dated to earliest Miocene from sediment infill (e.g., Comas et al., 1999; Do Couto et al., 2016), or latest Oligocene from basement studies (Booth-Rea et al., 2004b; Garrido et al., 2011). Previous works interpreted the end of extension during the late Tortonian (e.g., Martínez-García et al., 2017), although our work supports that some extension continued into the Messinian. However, the end of the extension may not be synchronous across the entire system. Post-Messinian evolution is characterized by contractional reorganization with faults accommodating African-Iberian NW plate convergence. Most of these structures, such as the Carboneras and Palomares fault systems initiated in the latest Miocene or early Pliocene times, leading to the contractional reorganization of the basin during the Pliocene-Holocene (Gràcia et al., 2006, 2019; Moreno et al., 2016; Gómez de la Peña et al., 2016). A similar basin re-structuration with inversión of previous extensional faults appears to have occurred across the entire West Mediterranean (Zitellini et al., 2020; Camafort et al., 2020a, 2020b).

6.2. Review of proposed geodynamic models

We summarize the geodynamic evolution of the Western Mediterranean so far proposed in 8 main models (Table 3), which can be gathered in three groups (Fig. 25; Chertova et al., 2014a).

6.2.1. North-dipping continuous slab

This group of models proposes an initial north-dipping subduction zone south of the Balearic Islands, which evolves as a continuous subduction zone (Fig. 25a). From Oligocene times Model 1 trench migrated southward and westward acquiring an arcuate shape by the early Miocene (Jolivet et al., 1999; Jolivet and Faccenna, 2000; Jolivet et al., 2009). Extension in the Alboran Basin started between 30-23 Ma (late Oligocene) (Jolivet and Faccenna, 2000), and at ~5 Ma the deformation front is located near its present-day position. Model 2 subduction front is initially longer than in Model 1, extending further north (Rosenbaum et al., 2002). The trench migrates southwards until the late Oligocene, when westward directed rollback causes extension and magmatic activity in the Alboran Basin starting in Late Burdigalian. The subduction front reached its current position in the Tortonian, and extension ceased, although volcanism remained

active into the Messinian. Model 3 is similar to Model 1 but integrates slab windows to explain anorogenic volcanism (Faccenna et al., 2004, 2014). Model 4 focuses on the WAB to propose that subsidence initiated in the late Oligocene, and that the arcuate WAB-MB shape developed in Serravallian-Tortonian time, with extension and volcanism stopping in Tortonian time (do Couto et al., 2016).

6.2.2. North-dipping discontinuous slab

These models also start with a north-dipping subduction zone, but restricted to south of the Balearic Islands. Lithospheric tearing compartmentalized the slab evolution (Fig. 25b). Model 5 uses mantle tomography (Carminati et al., 1998; Wortel and Spakman, 2000) to propose an initial subduction front (~500 km long) that migrated first southward and later westward, opening the South Balearic and Alboran Basins (Spakman and Wortel, 2004). A 3D reconstruction infers that the opening of the Alboran Basin occurred ~25 Ma ago (latest Oligocene) (Chertova et al., 2014b). The subduction front is bounded by slab tears along the North African margin and Balearic Islands, which allow horizontal displacement of the different crustal domains and lateral influx of the asthenosphere. Model 6 invokes onland allochthonous terranes distribution to infer a southward, and later westward motion of a segmented slab (van Hinsbergen et al., 2014). The Alboran Basin formed at ~21 Ma (early Miocene), when the subduction front developed an arcuate shape with the southern and western flanks as subduction zones, while the northern flank is a transform boundary. At 16 Ma (Langhian), a collision with North Algeria, forms the Kabylides and Tell belts, which triggers transform lithospheric-fault formation south of the subduction front, limiting active subduction to the western section (Fig. 25b).

6.2.3. South-dipping and North-dipping slabs

The models focus on land geology and assume a segmented Tethyan slab with different sections that evolve independently. A south-dipping subduction in NW Africa is separated by a transform fault from a north-dipping slab under the Balearic promontory (Fig. 25c). Model 7 proposes a first Cretaceous-Paleogene subduction, followed by terrane collision during the early Oligocene and initial opening of the basins in thelate Oligocene. The Alboran slab retreats north-westward and later westward (Gelabert et al., 2002). Model 8 proposes a SE-dipping subduction that migrates northward to later rotate to E-dipping subduction that retreats westward (Vergés and Fernàndez, 2012). Subduction initiates in the Cretaceous, with Tethys slab subducting under the North African margin until middle Eocene (~47 Ma). The Alboran Basin opens at ~27 Ma (late Oligonece). At ~5 Ma, extension stopped and compressional deformation initiates. Calk-alkaline volcanism occurs during active subduction, and alkaline volcanism is not discussed.

6.2.4. Discussion of models and synthesis

No existing model explains all available observations (Table 3). North-dipping continuous slab models (section 6.2.1) are broadly consistent with magma distribution and geochemistry, and with timing of extension and contractive reorganization. However, this category of models cannot explain either the offshore sub-basins evolution or the mantle structure. These models mainly consider land data and do not integrate marine data and basin evolution (Models 1, 2, and 3), or only integrate local offshore observations (Model 4). Model 3 integrates upper-mantle tomography, but the limited resolution does not constrain slab discontinuities. A northward-dipping continuous slab is inconsistent with (i) a segmented slab supported by recent tomography (e.g., Fitschner and Villaseñor 2015); (ii) the southeastwards plunging of the Iberian lithosphere (Mancilla et al., 2015); and (iii) the metamorphic rocks distribution along the North African margin, as these models propose a continuous collision front along this margin.

Volcanic activity is commonly not integrated, and only Model 3 integrates that information in the reconstruction (Table 3).

Models with segmented slabs are supported by improvements in the resolution of the upper-mantle tomographic images (Section 6.2.2). Late-stage volcanism related to asthenospheric influx appears a consequence of lithospheric tearing, and lateral changes in crustal domains are explained by the presence of lithospheric structures. A discontinuous subduction front may explain the metamorphic rock distribution and crustal thickness variations along North Africa, where evidences of collision and transpression exist at the Rif (NW Morocco), the Temsamane units and the eastern Kabylides (N. Algeria) (Caby et al., 2014; Jabaloy-Sánchez et al., 2015; Bruguier et al., 2017). However, the geometry of subduction along the North African margin is not yet certain. The main observables not fully explained by these models are (i) the SE dipping Iberian slab under the Alboran Domain (Mancilla et al., 2015), as the initial subduction is north-directed; and (ii) not integrated evolutionary aspects of the Alboran Basin. The fore-arc WAB-MB location and curved shape is not coherent with the west directed subduction geometry proposed in these models for the Gibraltar Arc. These models integrate the opening of the basins but do not discuss the end of extension offshore.

Finally, models that infer a segmented slab initially dipping towards the south in the westernmost Mediterranean explain the images of the Iberian SE dipping slab (Mancilla et al., 2015). Although the dynamics of the subduction zone are similar in both models, Model 8 (Vergés and Fernàndez, 2012) includes lithospheric tears, while Model 7 (Gelabert et al., 2002) does not consider slab segmentation. A south-dipping segmented slab appears coherent with the recent models of slab structure (Fichtner and Villaseñor, 2015), with the crustal domains distribution, and with the collisional events recorded in the North African margin. Nonetheless, upper mantle tomography is poorly constrained under north Africa, due to the sparse seismic station coverage compared to southern Europe. These models, however, assume several poorly documented aspects (Table 3): (i) subduction initiation in Cretaceous-middle Paleogene time is not clearly supported by recent observation; (ii) volcanic affinity is partially integrated — the model does not exclude lithospheric detachment below the Betics or Rif, which may explain the alkaline volcanism, although such scenario is not discussed in a largely 2D model; and (iii) marine data were not integrated in detail, so 3D basin evolution is not discussed. The end of extension in Model 8 is coherent with contractional reorganization at ~5 Ma.

7. The western Mediterranean evolution

We propose a revised kinematic model of the evolution of the westernmost Mediterranean that integrates the evolution of the marine sub-basins to refine the existing models (Fig. 26). The arcuate shape of the WAB-MB fore-arc basin supports a northwestward migration of the basins during the early Miocene, in agreement with models that propose a northwestwards retreat of a south-dipping slab followed by a late Miocene westward migration. The oldest two sub-basins, WAB-MB and HBB-PB, formed above pre-Miocene metamorphic basement (WAB-MB and HBB-PB), whereas the SAB, EAB and the NE Alboran sub-basins developed above volcanic basement, mainly generated during Tortonian times. The generation of oceanic and magmatic-arc crust implies significant horizontal displacement of pre-existing basins (Fig. 26a-e).

Based on our analysis, the evolution of the westernmost Mediterranean basin can be divided into two main stages: 1) The **formation stage**, during latest Oligocene to late Miocene times, in which the region evolved in a dominantly extensional setting kinematically linked to subduction-related slab rollback and when the sub-basins described in this work developed, and 2) A younger **contractive inversion stage** that

propagated in time and space from latest Miocene to Quaternary times, which we interpret as controlled by the NW-SE convergence between the African and European tectonic plates rather than being subduction–driven, that is active in the entire west Mediterranean (e.g., Camafort et al., 2020b). Evidence of this younger phase are currently active structures like Yusuf and Carboneras Fault Systems and the Alboran Ridge, which support a contractive reorganization of the westernmost Mediterranean beginning in latemost to post-Messinian times (e.g., Gràcia et al., 2006, 2012, 2019; Martínez-García et al., 2013; d'Acremont et al., 2020). Sedimentary units differ among sub-basins until the latest Messinian, changing to a common region-wide depositional system afterwards.

Our reconstruction starts in the early Miocene, corresponding to the oldest little-deformed offshore drilled sediments. During Aquitanian or perhaps Burdigalian times, Unit VII was deposited in the WAB, MB, and currently emerged Betic sub-basins (BB) (Fig. 26a) in restricted basement depocenters. These oldest sedimentary units support that rollback started at these times (Rosenbaum et al., 2002). The position of the WAB-MB-BB during the basins opening time should be restored towards the east, a distance equivalent to the extension in the back-arc, which presently is not well constrained (e.g., Faccenna et al., 2004), plus the new crust of the magmatic-arc. Considering the width of the newly-created magmatic-arc crust, this distance is at least of ~300 km, without including back-arc extension. Due to the WAB-MB-BB arcuate shape and widening of depocenters over time, we support a north-west directed migration of the slab turning to a later westward retreat. We locate the subduction front based on the WAB-MB-BB geometry, as this sub-basin was developed behind the subduction front. Based on their present-day relationship to the slab, we assume they were above the slab hinge, although the distance between the depocenters and the subduction front is not well constrained because it depends on the dimensions of the contractional frontal structures at each age step. The WAB and MB lack of visible extensional faulting in basement and sediments, and the deposits indicate vertical subsidence, which might have been driven by the density anomaly generated by the sub-vertical slab below these fore-arc basins (Ranero et al., 2000; Fig. 24). The continuity of the Ronda and Beni Bousera peridotites below the WAB supports a very thin continental basement under the WAB-MB (Guerdaoui et al., 2019), which may have contribute to thesubsidence. We infer for the BB Miocene marine depocenters a tentative position, north of the WAB-MB depocenter (Fig. 26a). The exact relative position of these sub-basins is difficult to restore, due to the later compartmentalization and deformation affecting them. The metamorphism of the Temsamane units in north Morocco (33–13 Ma, Booth-Rea et al., 2012, Jabaloy-Sánchez et al., 2015) may support an early Miocene transpressive zone along the North African margin (currently located within the eastern Rif), tentatively displayed in grey in Figure 26a.

During the Langhian–Serravallian times, sedimentation in the WAB-MB-BB indicates regional changes. The WAB widened in a W-E direction, while the width of the MB (W-E oriented) remained constant, indicating a change in dynamics, probably related to the change of subduction direction towards the west (Fig. 26a-b). Langhian–Serravallian sediments are the first in the HBB-PB, indicating the development of a new depocenter (Fig. 26b). While no signs of Langhian–Serravallian deformation are recorded in the WAB-MB, the pre-Messinian HBB-PB sequence is folded (Figs. 18 CMP 7000-2000, 19c). Deformation of pre-MSC units in the continental platform of eastern Algeria has been explained by the collision of the subduction front with the north African margin (Bouyahiaoui et al., 2015). However, that type of deformation does not extend into the westernmost basins (Strzerzynski et al., 2010; Badji et al., 2015; Bouyahiaoui et al., 2015). The lack of significant Serravallian compressional deformation on land in the HBB-PB area supports a different origin for the pre-MSC sediment deformation. The pattern of the deformation supports that a transcurrent fault-system bounded the HBB-PB (Fig. 26b). The HBB-PB are

located on the North African continental shelf, and their position through time has been reconstructed based on paleo-tectonic reconstructions of the North African coastline (Mazzoli and Helman, 1994; Gueguen et al., 1998, Fig. 26a, b). The exact position of the Langhian–Serravallian WAB-MB depocenters is not well constrained, but can be inferred from the amount of extension in the arc and the back-arc. The different seismic units identified and the different metamorphic crustal domains (Gómez de la Peña et al., 2018) between the WAB-MB and the HBB-PB supports that they were separated by major tectonic structures allowing the westward migration of the WAB-MB continental block with respect to the North African continental crust, which contained the HBB-PB. Thus, the HBB-PB probably originated by the transtensional stresses related to this major strike-slip lithospheric boundary during the westward migration of the Alboran Domain. These transtensional processes affecting the North African margin are consistent with observations on land, describing Tortonian extensional detachments in relation to a subduction transform setting (Booth-Rea et al., 2012).

In the early Tortonian (Fig. 26c), the beginning of magmatic activity implies the creation of new areas with a volcanic basement as part of the volcanic arc (EAB) and back-arc (ABB), which led to the creation of new sedimentary depocenters. Volcanic activity led to the formation of the Djibouti Plateau, the SAB and EAB basements, and the basement of the Carboneras Fault area, almost completed by the late Tortonian (Fig. 26d). The opening of the arc and back-arc regions is roughly coeval to the exhumation of the Temsamane units onshore (inset Fig. 1), and affected by extensional detachments dated as Tortonian (~11–7 Ma) (Negro et al., 2008; Jabaloy-Sánchez et al., 2015; Azdimousa et al., 2018).

The end of significant volcanism and beginning of sedimentation associated to dominant subaerial-erosion in these new areas started in the latest Tortonian–Messinian (Fig. 26d, e). Tortonian units are different among the new depocenters. They are ≤ 0.5 s TWTT thick and have intercalated volcanic layers in the SAB, EAB, and HBB-PB sub-basins, and are much thicker in the WAB-MB, related to an important subsidence pulse in this depocenter. In the HBB-PB, subsidence continued during the Tortonian, but it was subdued and restricted to narrow depocenters. It is inferred that extension at the ABB stalled. The position of the deformation front at 9 Ma times has been reconstructed by on-land paleomagnetic data (Crespo-Blanc et al., 2016).

Messinian sediments occur across most of the region and filled-up the existing sub-basins. Although subsidence appears to diminish in sub-basins and sedimentation extends out of the depocenters, sediment facies remain different among depocenters. In much of the WAB-MB, Messinian sediments appear as thin discontinuous deposits with a chaotic structure. In the SAB and the western side of the EAB, this unit is similar to the WAB, but with more continuous deposits. In the EAB, HBB and PB, Messinian units thicken to ≤ 1.5 s TWTT. The eastern part of the EAB and in the ABB the Messinian largely consists of evaporites, that are not imaged to the west (Figs. 8c-d, 21b). The top of the Messinian (M reflection) appears different for each sub-basin. Late Messinian units onlap the individual constructions of the volcanic arc like ridges, indicating that by the end of the Messinian volcanic arc activity terminated.

During the late Miocene-early Pliocene to recent, the southern sector of the Iberia Peninsula was progressively uplifted in relation to the slab tearing or detachment under the Betics (Garcia-Castellanos and Villaseñor, 2011; Mancilla et al., 2015). During the uplift, possibly much of the emerging marine Miocene sediments were eroded and currently, only the deepest depocenters are preserved along much of the Betics, indicating that the original width of the basin was considerably larger (Figs. 1b and 26e-g).

The first deposit with a distribution not associated to local subsidence or volcanic basement growth is Pliocene–early Pleistocene Unit II (Fig. 26f). Subsidence analysis of wells in the north margin of the

Alboran Basin show that subsidence extended towards the eastern basin in the Zanclean (Docherty and Banda, 1995). In agreement, Unit II extends across the entire deep basin displaying similar facies. The change in subsidence is coeval to changes of slab dynamics described for late Messinian time (e.g., Iribarren et al., 2007). We interpret that the change in subsidence is related to a stalling of slab migration, perhaps related to the slab detachment under the eastern Betics. This change, together with the wanning of magmatic activity (Duggen et al., 2004, 2008) led to thermal subsidence of the whole region, and may explain the similar basin-wide subsidence.

The latest Miocene change in stress configuration initiated a phase of shortening mostly accommodated along a few major tectonic structures, probably re-using previous tectonic domain boundaries (Gómez de la Peña et al., 2018; Gràcia et al., 2019) (Fig. 26e-g). These are the Carboneras Fault system (Gràcia et al., 2006, 2012; Moreno, et al., 2016), the Al-Idrissi Fault system (Martínez-García et al., 2013; Lafosse et al., 2016; Medina and Cherkaoui, 2017; Gràcia et al., 2019), the Alboran Ridge Fault system (Martínez-García et al., 2013, 2017) and the Yusuf Fault system (Alvarez-Marrón, 1999; Martínez-García et al., 2011, 2013, 2017). Shortening in the Alboran basins probably propagated from east to west, with evidence of shortening onshore in the Eastern Betic basins and the Palomares margin during the latest Tortonian (~8 Ma) (De Larouzière et al., 1988; Booth-Rea et al., 2004a; Giaconia et al., 2015). Structures further west, such us the Alboran Ridge and the Yusuf fault systems initiated their activity later during the latest Messinian to Zanclean. The lack of compressive structures in contemporary sedimentary basins suggests that the main deformation focused along those few crustal-scale structures (Gómez de la Peña et al., 2018). During the Pliocene-Holocene period, the Alboran Ridge and the Yusuf fault systems accommodated a NW-SE shortening estimated at ~20–30 km (Gómez de la Peña, PhD Thesis, 2017). Due to the activity of the Yusuf and Alboran Ridge fault systems, the HBB and PB were displaced towards the NW during the Pliocene-Holocene (Fig. 26e-g).

In summary, differences in stratigraphy and tectonic structure supports individual evolution of sub-basins until the Messinian time, and a younger common evolution for the whole region after its transformation into a single basin. While Miocene depocenters appear related to arc and back-arc extension and fore-arc subsidence, Pliocene-Holocene unit deposition appears controlled by basin-wide subsidence and conditioned by local contractional to strike-slip fault systems .

8. Conclusions

We provide the first basin evolution study for the westernmost Mediterranean. The region is characterized by several large depocenters that formed on different types of basement and had a distinct evolutionary history during the Miocene. In contrast, the entire region has a similar Pliocene-Holocene tectonic and stratigraphic evolution.

Extension in the Alboran Basin initiated in the Chattian–Burdigalian and continued until the Messinian. The first sediments in the Algero-Balearic Basin are late Miocene (possibly Tortonian) in age, although Messinian salt obscures images of the older stratigraphy. During the latest Miocene,regional extension stopped, evolving since then to a compressive setting, although not synchronously in all the basin. The Miocene compartmentalized subsidence, crustal domains distribution, and Pliocene-Holocene contractional structures help to understand the approximate position of the depocenters through time.

The oldest depocenter is the WAB-MB (Aquitanian-Burdigalian), including marine basins currently found onshore in the Betics. The WAB-MB may have initiated in a position some 300 km eastwards of its current

location. The lack of extensional structures in the WAB-MB depocenter, together with its position above the slab hinge, suggests a subsidence evolution model in a fore-arc setting for this basin.

The subsequently created depocenter is the HBB-PB (Langhian). The HBB-PB strata are folded and separated from the WAB-MB depocenter by a major lithospheric-scale strike-slip fault. This boundary accommodated the westward motion of the WAB-MB allowing the independent evolution of both areas, and provided a transtensional regime forming the HBB-PB depocenter.

The development of a volcanic arc basement formed new sedimentary depocenters that record an initiation in Tortonian time at the central, eastern and northeastern Alboran Basin. Extension in the back-arc created new oceanic crust at the ABB. Meanwhile, subsidence in the WAB-MB and the HBB-PB depocenters continued.

Each depocenter evolved independently until the Messinian. A change in deposition occurred near the Miocene-Pliocene transition. The Miocene sediment units were restricted by basement depocenters, but Pliocene-Holocene sedimentary units are widespread across the entire basin. Marine sedimentation on the BB only continues in the depocenters closest to the coast. The Pliocene-Holocene is characterized by contractional deformation mainly accommodated by re-activation of pre-existing crustal structures separating basement domains, such as Carboneras, Yusuf and the Alboran Ridge Fault Systems.

Different geodynamic models of the westernmost Mediterranean evolution fail to explain the marine basin evolution. The most suitable group of models include a discontinuous slab that migrated westward during the middle to late Miocene. The geometry of the subduction front should be coherent with the arcuate shape of the WAB-MB depocenter. Based on our observations, we propose a refined kinematic model of the westernmost Mediterranean (Fig. 26) that integrates basin evolution from the earliest Miocene to the present-day.

Acknowledgements:

The authors acknowledge support from the Spanish Ministry of Economy and Competitiveness through the Complementary Action ESF TopoEurope TOPOMED (CGL2008-03474-E/BTE), national projects EVENT (CGL2006-12861-C02-02), INSIGHT (CTM2015-70155-R), FRAME (CTM-2015-71766-R), LITHOSURF (CGL2015-67130- C2-1-R) and COST Action 1301 “FLOWS.” This work was supported by the Spanish Ministry of Education, Culture and Sport through the FPU fellowship 2013–2017 to L. Gómez de la Peña (AP2012-1579), and benefitted from a Marie Skłodowska-Curie Individual Fellowship to L. Gómez de la Peña (H2020-MSCA-IF-2017 796013). C. R. Ranero is funded by the Spanish Science and Innovation Ministry project FRAME CTM2015-71766-R, E. Gràcia is funded by the Spanish Science and Innovation Ministry project “STRENGHT” PID2019-104668RB-I00, and G. Booth-Rea through the Spanish Science and Innovation Ministry project PID2019-107138RB-I00 and the “Junta de Andalucia” project P18-RT-36332. This work has been carried out within Grup de Recerca Consolidat de la Generalitat de Catalunya “Barcelona Center for Subsurface Imaging” (2017 SGR 1662).

Figure captions:

Figure 1: (a) Regional bathymetric map of the Alboran Sea compiled using the swath-bathymetric data acquired during the IMPULS-06, EVENT-10, TOPOMED-11, SHAKE-15 and IDRISSI-16 marine cruises (e.g., Gràcia et al., 2006, 2012) and the existing datasets from "*Instituto Español de Oceanografía*" (IEO, Ballesteros et al., 2008, Gómez de la Peña et al., 2016) and GEBCO. Land topography is from the SRTM-3 grid. Main tectonic structures are displayed (Gràcia et al., 2019). AIF: Al-Idrissi Fault System, ARF: Alboran Ridge Fault System, CF: Carboneras Fault System, PF: Palomares Fault System, YF: Yusuf Fault System. Inset: Main tectonic units of the Westernmost Mediterranean with the location of the studied area boxed in red (modified from Gómez de la Peña et al., 2018). The current location of the AlKaPeCa terrains is shown, as well as a sketch of the Tethys subducion front. ABB: Algero-Balearic Basin, Alb: Alboran Basin, BBP: Beni-Bousera Peridotites, GC: Gulf of Cadiz, Guad. Basin: Guadalquivir Basin, Lig.: Ligurian Basin, RP: Ronda Peridotites, Tyr.: Tyrrhenian Basin. **(b)** Location of MCS profiles, commercial and scientific wells and dredges (see map legend with the details). The location of the figures is shown (red and yellow lines). Red numbers depicted the location of the main sedimentary depocentres onshore the Betics: 1: Fortuna Basin, 2: Lorca Basin, 3: Mazarrón Basin, 4: Vera Basin, 5: Tabernas-Sorbas Basins, 6: Níjar Basin, 7: Baza Basin, 8: Guadix Basin, 9: Granada Basin, 10: Malaga Basin.

Figure 2: (a) Depth migration of profiles CAB-104, parallel to the SE margin, and **(b)** CAB-125, perpendicular to the margin (modified from Booth-Rea et al., 2018). Along these profiles, is well notice how the Messinian top is a paraconformity along most of Iberian continental slope, while is an unconformity in areas disturbed by mud diapirism. Most of the unconformities are intra-Pliocene. The cross point of the two profiles, as well as the projected position of the DSDP-121 well are shown. See Figure 1a for location. Age of the units is defined in Figure 3.

Figure 3: (a) Ages and seismostratigraphic units identified in the Alboran Basin. Each column in the table represents a geographical area: WAB: West Alboran Basin, MB: Malaga Basin, SAB: South Alboran Basin, N. AR: North Alboran Ridge (Alboran Channel), EAB: East Alboran Basin, ABB: Algero-Balearic Basin and HBB: Habibas Basin. Limits between units are displayed in the same colour as the respective horizon at the seismic profiles. Red wavy lines represent unconformities. (b-g) Examples of the seismic facies found at **(b)** the West Alboran Basin (WAB), **(c)** the South Alboran Basin (SAB), **(d)** northern Alboran Ridge, **(e)** the western East Alboran Basin (EAB), **(f)** the eastern East Alboran Basin and the Algero-Balearic Basin (ABB) and **(g)** the Habibas and Pytheas basins (HBB and PB) (see Figure 1b for location). c: chaotic deposits, UU: Upper Unit, MU: Mobile Unit, LU: Lower Unit. TS: Top surface, BS: Bottom surface, M: Messinian top reflection, vA: volcanic unit in Alboran Ridge area, vY: volcanic unit in Yusuf Fault area, vD: volcaniclastic unit in Djibouti plateau area. Mt. B: Metamorphic basement, Mg. B: Magmatic basement. Correlation with ODP Leg 161 sites and HBB-1 is displayed.

Figure 4: Correlation between the seismostratigraphic units defined in this article (colored columns) and the previous units defined in the Alboran Basin depocenters. The correlation is organized by basins, starting from the WAB–MB (West Alboran and Malaga basins) (left panels), compared to Jurado and Comas 1992 (J&C, 92), Soto et al., 2012 (S, 2012) and Do Couto et al., 2016 (DC, 2016) units. In the central panels are the SAB (South Alboran Basin), N.AR (North Alboran Ridge) and EAB (East Alboran Basin) areas, compared to the Martínez-García et al., 2013 (MG, 2013), Juan et al., 2016 (J, 2016), Álvarez-Marrón, 1999 (AM, 1999), Booth-Rea et al., 2007 (BR, 2007) and Giaconia et al., 2015 (G, 2015) units. Finally, in the right section are the units of the HBB and PB, compared with the units proposed by Medaouri et al., 2014 (M, 2014). The wavy red lines depict the inferred erosive unconformities from the mentioned studies.

Figure 5: Stratigraphic column of the eastern Betic basins, representative of the Vera, Sorbas, Níjar and Tabernas basins (see Figure 1b for location). Modified from Giaconia et al., 2014.

Figure 6: Time migration of profiles EVDT1-3B **(a),** EVDT1-3A **(b)** and TM16 **(c),** parallel to the SAB depocenter (Fig. 1b). Main structures and seismostratigraphic units are identified. Age of the units is defined in Figure 3, and location of ODP Leg 161 site 979 is shown. Vertical exaggeration is of ~x:2.5 applying a 2100 m/s velocity, suitable for the sediments.

Figure 7: Time migration of profiles **(a)** TM05, **(b)** TM04 and **(c)** TM03, perpendicular to the SAB depocenter (see location in Figure 1b). These profiles record the Alboran Ridge uplift in the Pliocene-Holocene units, shown by the wedge of sediments displayed on the flank of the Alboran Ridge. Main structures and seismostratigraphic units are identified. Age of the units is defined in Figure 3. Vertical exaggeration is of ~x:2.5 using a 2100 m/s velocity, suitable for the sediments.

Figure 8: Time migration of profiles **(a)** TM11, **(b)** TM12, **(c)** TM13, and **(d)** TM14, running perpendicular to the Yusuf Fault in the EAB (Fig. 1b). These profiles show transition from the EAB to the ABB, where Messinian evaporites are imaged. The base of the MU (salt unit) is an inverse polarity reflection (Figs. 8c CMPs 9250-13000, 8d CMPs 5000–8500) that acts as *décollement* surface to the overlying material and causes normal faulting of units I and II (Fig. 8c CMPs 9250–1000). Main structures and seismostratigraphic units are identified. Age of the units is defined in Figure 3, and location of ODP Leg 161 site 977 is shown. Vertical exaggeration is of ~x:2.5 taking into account a 2100 m/s velocity, suitable for the sediments. B: basement.

Figure 9: Time migration of profile ESCI-Alb1 (see location in Figure 1b). Main structures and seismostratigraphic units are identified. Age of the units is defined in Figure 3. Vertical exaggeration is of ~x:2.5 taking into account a 2100 m/s velocity, suitable for the sediments.

Figure 10: Time migration of profile TM28 (see location in Figure 1b). Main structures and seismostratigraphic units are identified. Age of the units is defined in Figure 3. Vertical exaggeration is of ~x:2.5 using a 2100 m/s velocity, suitable for the sediments.

Figure 11: Time migration of profile TM22 (see location in Figure 1b). This profile is divided in **a)** Western section and **b)** Eastern section. Main structures and seismostratigraphic units are identified. Age of the units is defined in Figure 3. Vertical exaggeration is of ~x:2.5 considering a 2100 m/s velocity, suitable for the sediments

Figure 12: Time migration of profile TM29 (see location in Figure 1b). This profile is divided in **a)** Western section and **b)** Eastern section. Age of the units is defined in Figure 3. ODP 976: ODP Leg 161 site 976. Vertical exaggeration is of ~x:2.5 considering a 2100 m/s velocity, suitable for the sediments.

Figure 13: Time migration of profile TM17 (see location in Figure 1b). This profile is divided in **a)** Northwestern section and **b)** Southeastern section. Main structures and seismostratigraphic units are identified. Age of the units is defined in Figure 3. Also are shown the location of DSDP 121 and ODP site 976 (Leg 161). Vertical exaggeration is of ~x:2.5 taking into account a 2100 m/s velocity, suitable for the sediments.

Figure 14: Time migration of profile TM19 (see location in Figure 1b). This profile is divided in **a)** Northwestern section and **b)** Southeastern section. Main structures and seismostratigraphic units are

identified. Age of the units is defined in Figure 3. Vertical exaggeration is of ~x:2.5 considering a 2100 m/s velocity, suitable for the sediments.

Figure 15: Time migration of profile TM21, running across the WAB in a SW-NE section (see location in Figure 1b). This profile is divided in **a)** Southwestern section and **b)** Northeastern section. Main structures and seismostratigraphic units are identified. Age of the units is defined in Figure 3. Vertical exaggeration is of ~x:2.5 taking into account a 2100 m/s velocity, suitable for the sediments.

Figure 16: Time migration of profile TM18 (see location in Figure 1b). This profile can be correlated with the Andalucia G-1 well (located northern) using the CAB cruise profiles (Fig. 1b), as due to the steepness of the margin the sedimentary thickness highly increases in N-S direction. Main structures and seismostratigraphic units are identified. Age of the units is defined in Figure 3. Vertical exaggeration is of ~x:2.5 considering a 2100 m/s velocity, suitable for the sediments.

Figure 17: Time migration of profile TM20 (see location in Figure 1b). Main structures and seismostratigraphic units are identified. Age of the units is defined in Figure 3. Vertical exaggeration is of ~x:2.5 using a 2100 m/s velocity, suitable for the sediments.

Figure 18: Time migration of profile TM15 (see location in Figure 1b). This profile runs across the HBB. Main structures and seismostratigraphic units are identified. Age of the units is defined in Figure 3. Vertical exaggeration is of ~x:2.5 considering a 2100 m/s velocity, suitable for the sediments. Mt.B.: metamorphic basement.

Figure 19: Time migration of profiles TM14 **(a)**, TM13 **(b)**, TM12 **(c)**, and TM11 **(d)** (see location in Figure 1b), running perpendicular to TM15 (Fig. 18). These profiles show the HBB variations from east to west. Main structures and seismostratigraphic units are identified. Age of the units is defined in Figure 3. Vertical exaggeration is of ~x:2.5 taking into account a 2100 m/s velocity, suitable for the sediments. Mt.B.: metamorphic basement, YF: Yusuf Fault.

Figure 20: Time migration of profiles TM15 **(a)** and TM09 **(b)** in the PB area (Fig. 1b). Main structures and seismostratigraphic units are identified. Age of the units is defined in Figure 3. Vertical exaggeration is of ~x:2.5 considering a 2100 m/s velocity, suitable for the sediments.

Figure 21: Time migration of profile TM23 (see location in Figure 1b) (modified from Gómez de la Peña et al., 2016). This profile is divided in **a)** Northwestern section and **b)** Southeaster section. The deeper parts of the profile are masked by the multiple energy. Main structures and seismostratigraphic units are identified. Age of the units is defined in Figure 3. Vertical exaggeration is of ~x:2.5 aplying a 2100 m/s velocity, suitable for the sediments.

Figure 22: SW-NE geological section of the Lorca Basin (see location in Figure 1b). The units are described in the color legend. Modified from Booth-Rea et al., 2004c.

Figure 23: Proposed interpretation for the late Miocene sediments at the WAB. **(a)** Un-interpreted and **(b)** interpreted sections of profile TM12 (see location in Figure 19c), running across the HBB (Fig. 1). **(c)** Un-interpreted and **(d)** interpreted sections of profile TM17 (see location in Figure 13a), across the WAB (Fig. 1). **(e)** Proposed interpretation of the same section of profile TM17, base on the similarities in the seismic expression of the late Miocene sediments of the HBB and the WAB.

Figure 24: a) Crustal configuration of the Gibraltar Arc System. The crustal thickness is shown where available, based on receiver function analysis (Mancilla et al., 2015) and Wide-Angle seismic data (Booth-Rea et al., 2018, Gómez de la Peña et al., 2020). Gray dots marked the location of the onshore stations used for the receiver funcions analysis, and yellow dots the location of the Ocean Bottom Hydrophones/Seismometers used in the Wide-Angle seismic data acquisition. The pink dotted line delimited the Alboran Domain allochthonous terrain extension. The red dotted-line englobes the magmatic-arc crust. A brown dotted line depicts the boundary between the Alboran and North African continental crusts. The volcanic outcrops are displayed (see legend for details). AIF: Al-Idrissi Fault, ARF: Alboran Ridge Fault, CF: Carboneras Fault, TF: Trougout Fault, YF: Yusuf Fault. **b and c)** Tomographic images showing the slab distribution at 100 and 300 km depth, respectively (modified from Chertova et al., 2014a).

Figure 25: Illustration of the three different subduction scenarios for the opening of the Alboran Sea (modified from Chertova et al., 2014a). **(a)** Long initial trench along the entire Gibraltar-Balearic margin (Rosenbaum et al., 2002; Faccenna et al., 2004; Jolivet et al., 2009; Do Couto et al., 2016). **(b)** Initial subduction zone near the Balearic Islands, north-dipping discontinuous slab (Spakman and Wortel, 2004; van Hinsbergen et al., 2014). **(c)** S-SE dipping initial subduction zone under North Africa (Gelabert et al., 2002; Vergés and Fernández, 2012).

Figure 26: Reconstruction of the Alboran Basin evolution based on the ages, distribution and deformation of the sedimentary units. Main depocenters and structures are shown (see figure legend for details). The African coastlines at 23 Ma (pink dash line) and at 10 Ma (orange dash line) are depicted as reference (Mazzoli and Helman, 1994; Gueguen et al., 1998). CF: Carboneras Fault, ARF: Alboran Ridge Fault, YF: Yusuf Fault, AIF: Al-Idrissi Fault. **(a) Burdigalian**. Only the WAB-MB-BB depocenter was created. The shape of this basin mimics the subduction front. **(b) Langhian-Serravallian**. Sedimentation at the WAB, MB and BB sub-basins continues, and the basin expands. A new depocenter, the HBB-PB, appears. The extensional directions change from NW-SE to E-W. A transform fault is inferred between these two depocenters, in order to allow the westward displacement of the subduction front. **(c) Early Tortonian**. The WAB-MB-BB depocenter continues travelling towards the west, following the slab rollback. First volcanic activity (red triangles) take place. **(d) Late Tortonian**. The magmatic activity in the area continues, creating a volcanic arc (volcanic outcrops are depicted with red polygons and the areas floored by volcanic basement are depicted with red lines). The extension in the arc and the westward migration of the subduction zone derives in a rapid migration of the WAB-MB-BB. At this time, the position of the subduction front and the WAB are well constrained on the basis of Crespo-Blanc et al. (2016) reconstruction. First sediments in the EAB, intercalated with volcanic layers, are identified, and probably oceanic crust is already created at the ABB. **(e) Messinian**. Extensional processes in the basin ceased. The volcanic activity in the basin finished, and main depocenters are already created. Contractive reorganization of the basin begins in some areas, as at the NE margin, where the Carboneras Fault starts its activity. **(f) Pliocene**. The general contractive reorganization of the basin occurred. The Yusuf Fault and the Alboran Ridge front fault begins to accommodate this convergence. Activity along these boundaries has a direct consequence the NW displacement of the SAB and the HBB-PB depocenters. Sedimentation is no more controlled by the subduction system and the basement distribution, and a Pliocene unit with similar characteristics over the entire region is observed. **(g) Quaternary**. The basin continues its evolution in this compressive setting, till acquired is current configuration. The Carboneras Fault, the Yusuf fault and the Alboran Ridge frontal fault are still active, and the Al-Idrissi fault appears. Sedimentation continues homogenous along the entire basin.

Table 1: Acquisition parameters for the new MCS data presented in this study. The total length of seismic profiles acquired in each survey is indicated.

Table 2: Processing flow applied to the TOPOMED, EVENT-DEEP and ESCI Alboran profiles (for further details, see Gómez de la Peña et al. (2018) supplementary material). Profiles TM23 and EVDT1-3A were processed in a different way. These two profiles (Figs. 6a and 21) were processed to study the sedimentary cover, and thus, multiple energy arriving later has not been removed. Seismic processing of these profiles included full streamer geometry, spherical divergence correction, normal-move-out correction based on velocity semblance analysis, stretching mute, amplitude recovery, time migration and a time and spatial variant band-pass filter.

Table 3: Comparison between the different models discussed and the data to fit. Nd: North directed, Sd: South directed.

		TOPOMED-GASSIS Leg 1	TOPOMED-GASSIS Leg 2	EVENTDEEP Leg1	EVENTDEEP Leg2	ESCI
	Profiles	TM01-TM25	TM26-TM30	EVD1-EVD4	EVD100-EVD211	Alb1
	km acquired	~1900 km	~650 km	~300 km	~1470 km	~90 km
Acquisition parameters	Number of active channels	408	480	96	276	180
	Distance between channels (m)	12.5	12.5	6.25	12.5	25
	Total streamer length (m)	5397	6332	600	3450	4500
	Streamer depth (m)	10	10	2.5	6	15
	Distance source-first channel (m)	150.8	203.7	45.6	114.0	120
	CMP distance (m)	6.25	6.25	3.125	6.25	12
	Sample rate (ms)	2	2	2	2	4
	Trace length (s)	12 / 14	19	3 / 3	12	22 / 18
	Shot distance (m)	37.5 / 50	50	12.5 18.75	37.5	50 / 75
	Air-guns depth (m)	7.5	9	2.5	6	7.5
	Air-guns volume (c.i.)	3060	4600	80	1880	7118

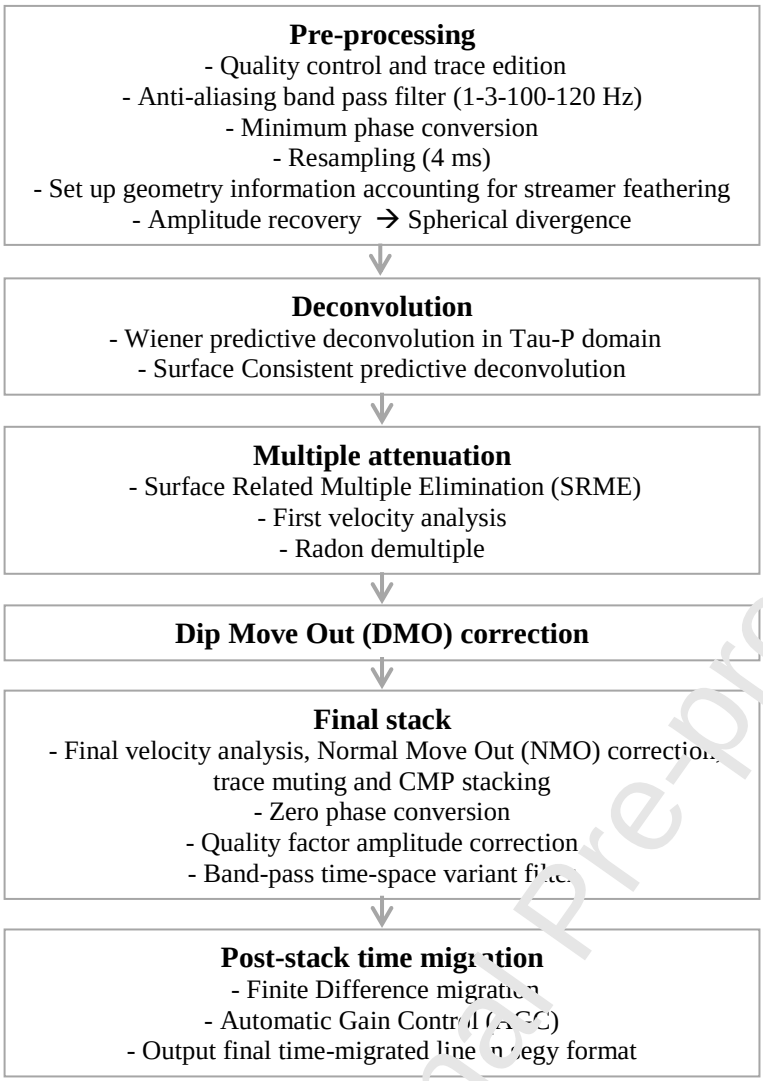

Data to fit	Geodynamic models							
	N directed (Nd) continuous slab				Nd discontinuous slab		Sd discontinuous slab	
	1	2	3	4	5	6	7	8
Slab distribution	Poor	Poor	Poor	Poor	Good	Good	Good	Good
Direction of subduction	Poor	Poor	Poor	Poor	Poor	Poor	Good	Good
Magma geochemistry	-	Fair	Good	-	Good	Good	-	Fair
Crust nature	Poor	Poor	Poor	Poor	Fair	Fair	Good	Good
Basin evolution	Poor	Poor	Poor	Poor	Poor	Poor	Fair	Fair
Pliocene reorganization	Good	Good	Good	Good	-	-	-	Good

References:

Aguado, R., Feinberg, H., Durand Delga, M., Martín Algarra, A., Esteras, M. and Didon, J., 1990. Nuevos datos sobre la edad de las formaciones miocenas trangresivas sobre las Zonas Internas Béticas: La Formación San Pedro de Alcántara (Provincia de Málaga): Rev. Soc. Geol. España, v. 3(1-2), p. 79-85.

Aïdi, C., Beslier, M., Yelles-Chaouche, A.K., Klingelhoefer, F., Bracene, R., Galve, A., Bounif, A., Schenini, L., Hamai, L., Schnurle, P., Djellit, H., Sage, F., Charvis, P., and Déverchère, J., 2018, Deep structure of the continental margin and basin off Greater Kabylia , Algeria – New insights from wide-angle seismic data: Tectonophysics, p. 728–729, doi: 10.1016/j.tecto.2018.01.007.

Alonso-Chaves, F.M., Andreo, B., Arias, C., Azañón, J.M., and Balanyá, J.., 2004, Cordillera Bética y Baleares, in Vera, J.A. ed., Geología de España, IGME, p. 347–464.

Alvarez-Marrón, J., 1999, Pliocene to Holocene structure of the Eastern Alboran sea (Western Mediterranean): Proceedings of the Ocean Drilling Program, Scientific Results, Vol. 161, v. 161, p. 345–355.

Aparicio, A., Mitjavila, J.M., Araña, V., and Villa, I.M., 1991, La edad del volcanismo de las islas Columbrete Grande y Alborán (Mediterráneo occidental): Boletín Geológico Minero, v. 102, p. 562–570.

Azañón, J.M., Crespo-Blanc, A., and García-Dueñas, V., 1997, Continental collision, crustal thinning and nappe forming during the pre-Miocene evolution of the Alpujarride Complex (Alboran Domain: Journal of Structural Geology, v. 19, p. 1055–1071, papers3://publication/uuid/2B1F8CE7-D05B-

476A-8D12-D44040472CBD.Azañón, J. M., A. Azor, G. Booth-Rea, and F. Torcal, 2004, Small-scale faulting, topographic steps and seismic ruptures in the Alhambra (Granada, southeast Spain), J Quaternary Sci, 19(3), 219-227.

Azañón, J., Galve, J., Pérez-Peña, J., Giaconia, F., Carvajal, R., Booth-Rea, G., Jabaloy, A., Vázquez, M., Azor, A. and Roldán, F., 2015, Relief and drainage evolution during the exhumation of the Sierra Nevada (SE Spain): Is denudation keeping pace with uplift? Tectonophysics, v. 663, p. 19-32.

Azdimousa, A., A. Jabaloy-Sánchez, P. Münch, J. M. Martínez-Martínez, G. Booth-Rea, M. Vázquez-Vílchez, L. Asebriy, J. Bourgois, and F. González-Lodeiro, 2018, Structure and exhumation of the Cap des Trois Fourches basement rocks (Eastern Rif, Morocco): J Afr Earth Sci, v. 150, p. 657-672. ff10.1016/j.jafrearsci.2018.09.018ff. ffhal01884964f

Badji, R., Charvis, P., Bracene, R., Galve, A., Badsi, M., Ribodetti, A., Benaissa, Z., Klingelhoefer, F., Medaouri, M., and Beslier, M.O., 2015, Geophysical evidence for a transform margin offshore Western Algeria: a witness of a subduction-transform edge propagator?: Geophysical Journal International, v. 200, p. 1027–1043, doi: 10.1093/gji/ggu454.

Balanyà, J.C., Crespo-Blanc, A., Díaz Azpiroz, M., Expósito, I., and Luján, M., 2007, Structural trend line pattern and strain partitioning around the Gibraltar Arc accretionary wedge: Insights as to the mode of orogenic arc building: Tectonics, v. 26, p. 1–19, doi: 10.1029/2005TC001932.

Ballesteros, M., Rivera, J., Muñoz, A., Muñoz-martín, A., Acosta, J., Carbó, A., and Uchupi, E., 2008, Alboran Basin, southern Spain — Part II: Neogene tectonic implications for the orogenic float model: Marine and Petroleum Geology, v. 25, p. 75–101.

Barragán, G., 1997, Evolución Geodinámica de la Depresión de Vera. Doctoral Thesis, Universidad de Granada, 300 pp.

Bezada, M.J., Humphreys, E.D., Toomey, D.R., Harnafi, M., Dávila, J.M., and Gallart, J., 2013, Evidence for slab rollback in westernmost Mediterranean from improved upper mantle imaging: Earth and Planetary Science Letters, v. 368, p. 51–60, doi: 10.1016/j.epsl.2013.02.024.

Blanco, M.J., and Spakman, W., 1993, The P-wave velocity structure of the mantle below the Iberian Peninsula: evidence for subducted lithosphere below southern Spain: Tectonophysics, v. 221, p. 13–34, doi: 10.1016/0040-1951(93)90025-F.

Booth-Rea, G., Azañón, J.M., Garcia-Dueñas, V., and Augier, R., 2003, Uppermost Tortonian to Quaternary depocentre migration related with segmentation of the strike-slip Palomares Fault Zone, Vera Basin (SE Spain): Cr Geosci, v. 335(9), p. 751-761.

Booth-Rea, G., Azañón, J.M., Azor, A. and García-Dueñas, V., 2004a, Influence of strike-slip fault segmentation on drainage evolution and topography, a case study: the Palomares Fault Zone (Southeastern Betics, Spain), European Geophysical Union (EGU), Nize.

Booth-Rea, G., Azañón, J.M., and García-Dueñas, V., 2004b, Extensional tectonics in the northeastern Bethics (SE Spain): Case study of extension in a multilayered upper crust with contrasting rheologies: Journal of Structural Geology, v. 26, p. 2039–2058, doi: 10.1016/j.jsg.2004.04.005.

Booth-rea, G. and Silva Barroso, P. G., 2004c, Mapa geológico de la Hoja nº 953 (Lorca). Mapa Geológico de la Región de Murcia. E 1:50.000. MGD 50. IGME

Booth-Rea, G., Azanon, J.M., Martinez-Martinez, J.M., Vidal, O. and V, G.D., 2005. Contrasting structural and P-T evolution of tectonic units in the southeastern Betics: Key for understanding the exhumation of the Alboran Domain HP/LT crustal rocks (western Mediterranean). Tectonics, 24(2), TC2009, doi:10.1029/2004TC001640

Booth-Rea, G., Ranero, C.R., Martínez-Martínez, J.M., and Grevemeyer, I., 2007, Crustal types and Tertiary tectonic evolution of the Alborán sea, western Mediterranean: Geochemistry, Geophysics, Geosystems, v. 8, Q10005, doi: 10.1029/2007GC001639.

Booth-Rea, G., Jabaloy-Sánchez, A., Azdimousa, A., Asebriy, L., Vílchez, M.V., and Martínez-Martínez, J.M., 2012, Upper-crustal extension during oblique collision: The Temsamane extensional detachment (eastern Rif, Morocco): Terra Nova, v. 24, p. 505–512, doi: 10.1111/j.1365-3121.2012.01089.x.

Booth-Rea, G., Martínez-Martínez, J.M., and Giaconia, F., 2015, Continental subduction, intracrustal shortening, and coeval upper-crustal extension: P-T evolution of subducted south Iberian paleomargin metapelites (Betics, SE Spain): Tectonophysics, v. 663, p. 122–139, doi: 10.1016/j.tecto.2015.08.036.

Booth-Rea, G., R. Ranero, C., and Grevemeyer, I., 2018, The Alboran volcanic-arc modulated the Messinian faunal exchange and salinity crisis: Scientific Reports, v. 8, p. 1–14, doi: 10.1038/s41598-018-31307-7.

Boullin, J., Bourgois, J., Chauve, P., Delga, M.D., Magne, J., Mathis, V., Peyre, Y., Riviere, M. and Vera, J.A., 1973, Lower Miocene Age of Formation of Vinuela, Inharmonious on Internal Betic Nappes (Malaga, Spain): Comptes Rendus Hebdomadaires Des Seances De L Academie Des Sciences Serie D, v. 276(8), p. 1245-1248.

Boullin, J. P., Durand-Delga, M., and Olivier, P., 1986, Betic Rifian and Tyrrhenian Arc: Distinctive features, genesis and development stages, in The Origin of Arcs, edited by F. Wezel, pp. 281–304, Elsevier, New York.

Bourgois J., Chauve P., Lorenz C., Monnot J., Peyre Y., Rjgo E. & Rwiere M. 1972, La formation d'Alozaina. Série d'age oligocène et aquitanien transgressive sur le Bètique de Malaga (région d'Alozaina-Tolox, province de Malaga, Espagne): Comptes rendus de l'Acaddmie des Sciences, Paris, v. 275, p- 531- 534.

Bousquet, J. C., 1979, Quaternary strike-slip faults in southeastern Spain: Tectonophysics, v. 52, p. 277–286.

Bouyahiaoui, B., Sage, F., Abtout, A., Klingelhoefer, F., Yelles-Chaouche, K., Schnürle, P., Marok, A., Déverchère, J., Arab, M., Galve, A., and Collot, J.Y., 2015, Crustal structure of the eastern Algerian continental margin and adjacent deep basin: Implications for late Cenozoic geodynamic evolution of the western Mediterranean: Geophysical Journal International, v. 201, p. 1912–1938, doi: 10.1093/gji/ggv102.

Braga, J.C., Jimenez, A.P., Martin, J.M. and Rivas, P. ,1996, Middle Miocene, coral-oyster reefs (Murchas, Granada, southern Spain). In: E. Franseen, M. Esteban, B. Ward y J.M. Rouchy (Editors).Braga, J.C., Martín, J.M., Wood, J.L., 2001, Submarine lobes and feeder channels of redeposited, temperate carbonate and mixed siliciclastic-carbonate platform-deposits (Vera Basin, Almería, southern Spain): Sedimentology v. 48, p. 99–116.

Braga, C., Martín, J.M. and Quesada, C., 2003, Patterns and average rates of late Neogene–Recent uplift of the Betic Cordillera, SE Spain: Geomorphology, v. 50, p. 3-26.Bruguier, O., Bosch, D., Caby, R., Vitale-Brovarone, A., Fernandez, L., Hammor, D., Laouar, R., Ouabadi, A., Abdallah, A., and Mechati, M., 2017, Age of UHP metamorphism in the Western Mediterranean: Insight from rutile and minute zircon inclusions in a diamond-bearing garnet megacryst (Edough Massif, NE Algeria): Earth Planet Sc Lett, v. 474, p. 215-225.

Butler, R. W., Pinter, P. R., Maniscalco, R., Hartley, A. J., 2020, Deep-water sand-fairway mapping as a tool for tectonic restoration: decoding Miocene central Mediterranean palaeogeography using the Numidian turbidites of southern Italy: Journal of the Geological Society, v. 177, p. 766-783.

Caby, R., Bruguier, O. Fernandez, L., Hammor, D., Bosch, D., Mechati, M., Laouar, R., Ouabadi, A., Abdallah, N., and Douchet, C. ,2014, Metamorphic diamonds in a garnet megacryst from the Edough Massif (northeastern Algeria). Recognition and geodynamic consequences: Tectonophysics, 637, 341-353.

Calvert, A., Sandvol, E., Seber, D., Barazangi, M., Roecker, S., Mourabit, T., Vidal, F., Algualcil, G., and Jabour, N., 2000, Geodynamic evolution of the lithosphere and upper mantle beneath the Alboran region of the western Mediterranean: Constraints from travel time tomography: Journal of Geophysical Research, v. 105, p. 10871–10898.

Camafort, M., Gràcia E., C.R. Ranero, 2020a, Quaternary seismo-stratigraphy and tectono-sedimentary evolution of the north Tunisian continental margin: Tectonics https://doi.org/10.1029/2020TC006243

Camafort M., J.V. Pérez-Peña, G. Booth-Rea, I. Melki, E. Gràcia, J.M. Azañón, J.P. Galve, W. Marzougui, S. Gaidi, C.R. Ranero, 2020b, Active tectonics and drainage evolution in the Tunisian Atlas driven by interaction between crustal shortening and mantle dynamics: Geomorphology, 351, https://doi.org/10.1016/j.geomorph.2019.106954

Cameselle A. L., Ranero C. R. Franke D., Barckhausen, U., 2017, The continent-ocean transition on the northwestern South China Sea: Basin Research, V. 29, pp 73-9.

Cameselle, A.L., and Urgeles, R., 2017, Large-scale margin collapse during Messinian early sea-level drawdown: The SW Valencia trough, NW Mediterranean: Basin Research, v. 29, p. 576–595, doi: 10.1111/bre.12170.

Carminati, E., Wortel, M.J.R., Spakman, W., and Sabadini, R., 1998, The role of slab detachment processes in the opening of the western-central Mediterranean basins: Some geological and geophysical evidence: Earth and Planetary Science Letters, v. 160, p. 651–665, doi: 10.1016/S0012-821X(98)00118-6.

Carminati, E., Lustrino, M., and Doglioni, C., 2012, Geodynamic evolution of the central and western Mediterranean: Tectonics vs. igneous petrology constraints: Tectonophysics, v. 579, p. 173–192, doi: 10.1016/j.tecto.2012.01.026.

Chalouan, A., and Michard, A., 2004, The Alpine Rif Belt (Morocco): A Case of Mountain Building in a Subduction-Subduction-Transform Fault Triple Junction: Pure appl. geophys., v. 161, 489-519 p., doi: 10.1007/s00024-003-2460-7.

Chalouan, A., Michard, A., El Kadiri, K., Negro, F., Frizon de Lamotte, D., Soto, J.I., and Saddiqi, O., 2009, The Rif Belt, in Continental Evolution: The Geology of Morocco. Lecture Notes in Earth Sciences, Springer-Verlat Berlin Heidelberg, doi: 10.1007/978-3-540-77076-3_5.

Chertova, M. V., Spakman, W., Geenen, T., van den Berg, A.P., and van Hinsbergen, D.J.J., 2014a, Underpinning tectonic reconstruction of the western Mediterranean region with dynamic slab evolution from 3-D numerical modeling: Journal of Geophysical Research, v. 119, p. 1–26, doi: 10.1002/2013JB010500.

Chertova, M. V., Spakman, W., van den Berg, A.P., and van Hinsbergen, D.J.J., 2014b, Absolute plate motions and regional subduction evolution: Geochemistry, Geophysics, Geosystems, p. 1–13, doi: 10.1002/2014GC005494.

Cifelli, F., Mattei, M., Rojas, I.M., Blanc, A.C., Comas, M., Faccenna, C. and Porreca, M., 2006, Neogene tectonic evolution of the Gibraltar Arc: New paleomagnetic constrains from the Betic chain: Earth and Planetary Science Letters, 250(3-4): 522-540.

Clauzon, G., Suc, J., Gautier, F., Berger, A., and Loutre, M., 1996, Alternate interpretation of the Messinian salinity crisis: Controversy resolved?: The Geological Society of America, v. 846, p. 363–366, doi: 10.1130/0091-7613(1996)024<0363.

Comas, M.C., García-Dueñas, V., and Jurado, M.J., 1992, Neogene Tectonic Evolution of the Alboran Sea from MCS Data: Geomarine Letters, v. 12, p. 157–164.

Comas, M.C., Platt, J.P., Soto, J.I., and Watts, A.B., 1999, 44. The origin and tectonic history of the Alboran Basin: Insights from leg 161 results: Proceedings of the Ocean Drilling Program, Scientific Results, v. 161, p. 555–580.

Corbi, H., Lancis, C., Garcia-Garcia, F., Pina, J.A., Soria, J.M., Tent-Manclus, J.E. and Viseras, C., 2012, Updating the marine biostratigraphy of the Granada Basin (central Betic Cordillera). Insight for the Late Miocene palaeogeographic evolution of the Atlantic - Mediterranean seaway. Geobios, v. 45(3): p 249-263.

Crespo-Blanc, A., Orozco, M. and Garcia-Dueñas, V., 1994, Extension Versus Compression during the Miocene Tectonic Evolution of the Betic Chain - Late Folding of Normal-Fault Systems: Tectonics, v. 13(1), p. 78-88.

Crespo-Blanc, A., and Frizon de Lamotte, D.F., 2006, Structural evolution of the external zones derived from the Flysch trough and the South Iberian and Maghrebian paleomargins around the Gibraltar arc: A comparative study: Bulletin de la Societe Geologique de France, v. 177, p. 267–282, doi: 10.2113/gssgfbull.177.5.267.

Crespo-Blanc, A., Comas, M., and Balanyá, J.C., 2016, Clues for a Tortonian reconstruction of the Gibraltar Arc: Structural pattern, deformation diachronism and block rotations: Tectonophysics, v. 683, p. 308–324, doi: 10.1016/j.tecto.2016.05.045.

d'Acremont, E., Lafosse, M., Rabaute, A., Teurquety, G., Do Couto, D., Ercilla, G., Juan, C., Mercier de Lépinay, B., Lafuerza, S., Galindo-Zaldívar, J., Estrada, F., Vazquez, J.T., Leroy, S., Poort, J., et al., 2020, Polyphase Tectonic Evolution of Fore - Arc Basin Related to STEP Fault as Revealed by Seismic Reflection Data From the Alboran Sea (W - Mediterranean): Tectonics, v. 39, p. 1–25, doi: 10.1029/2019TC005885.

de Larouzière, F. D., Bolze, J., Bordet, P., Hernandez, J., Montenat, C., and Ottd´Estevou, P., 1988, The Betic segment of the lithospheric Trans-Alboran shear zone during the Late Miocene:, Tectonophysics, v. 152, p. 41-52.

DeMets, C., Gordon, R.G., and Argus, D.F., 2010, Geologically current plate motions: Geophysical Journal International, v. 181, p. 1–80, doi: 10.1111/j.1365-246X.2009.04491.x.

Dewey, J.F., 1988, Extensional collapse of orogens: Tectonics, v. 7, p. 1123–1139, doi: 10.1029/TC007i006p01123.

Dewey, J.F., Helman, M.L., Knott, S.D., Turco, E., and Hutton, D.H.W., 1989, Kinematics of the western Mediterranean: Geological Society, London, Special Publications, v. 45, p. 265–283, doi: 10.1144/GSL.SP.1989.045.01.15.

Díaz, J., Gallart, J., and Carbonell, R., 2016, Moho topography beneath the Iberian-Western Mediterranean region mapped from controlled-source and natural seismicity surveys: Tectonophysics, v. 692, p. 74–85, doi: 10.1016/j.tecto.2016.08.023.

Do Couto, D., Popescu, S. M., Suc, J. P., Melinte-Dobrinescu, M. C., Barhoun, N., Gorini, C., ... & Auxietre, J. L., 2014, Lago Mare and the Messinian salinity crisis: evidence from the Alboran Sea (S. Spain): Marine and Petroleum Geology, v. 52, p. 57-76.

Do Couto, D., Gorini, C., Jolivet, L., Lebret, N., Augier, R., Gumiaux, C., d'Acremont, E., Ammar, A., Jabour, H., and Auxietre, J., 2016, Tectonic and stratigraphic evolution of the Western Alboran Sea Basin in the last 25Myrs: Tectonophysics, v. 677, p. 280–311, doi: 10.1016/j.tecto.2016.03.020.

Docherty, C., and Banda, E., 1995, Evidence for the eastward migration of the Alboran Sea based on regional subsidence analysis: A case for basin formation by delamination of the subcrustal lithosphere?: Tectonics, v. 14, p. 804–818.

Duggen, S., Hoernle, K., van den Bogaard, P., Rüpke, L., and Morgan, J.P., 2003, Deep roots of the Messinian salinity crisis.. Nature, v. 422, p. 602–606, doi: 10.1038/nature01553.

Duggen, S., Hoernle, K., van den Bogaard, P., and Garbe-Schönberg, D., 2005, Post-collisional transition from subduction- to intraplate-type magmatism in the westernmost Mediterranean: Evidence for continental-edge delamination of subcontinental lithosphere: Journal of Petrology, v. 46, p. 1155–1201, doi: 10.1093/petrology/egi013.

Duggen, S., Hoernle, K., van den Bogaard, P., and Harris, C., 2004, Magmatic evolution of the Alboran region: The role of subduction in forming the western Mediterranean and causing the Messinian Salinity Crisis: Earth and Planetary Science Letters, v. 218, p. 91–108, doi: 10.1016/S0012-821X(03)00632-0.

Duggen, S., Hoernle, K., Klügel, A., Geldmacher, J., Thirlwall, M., Hauff, F., Lowry, D., and Oates, N., 2008, Geochemical zonation of the Miocene Alborán Basin volcanism (westernmost Mediterranean): geodynamic implications: Contributions to Mineralogy and Petrology, v. 156, p. 577–593, doi: 10.1007/s00410-008-0302-4.

El Bakkali, S., Gourgaud, A., Bourdier, J.L., Bellon, H., and Gundogdu, N., 1998, Post-collision neogene volcanism of the Eastern Rif (Morocco): Magmatic evolution through time: Lithos, v. 45, p. 523–543, doi: 10.1016/S0024-4937(98)00048-6.

Estrada, F., Ercilla, G., and Alonso, B., 1997, Pliocene-Quaternary tectonic-sedimentary evolution of the NE Alboran Sea (SW Mediterranean Sea): Tectonophysics, v. 282, p. 423–442.

Estrada, F., Ercilla, G., Gorini, C., Alonso, B., Vázquez, J.T., García-Castellanos, D., Juan, C., Maldonado, A., Ammar, A., and Elabbassi, M., 2011, Impact of pulsed Atlantic water inflow into the Alboran Basin at the time of the Zanclean flooding: Geo-Marine Letters, v. 31, p. 361–376, doi: 10.1007/s00367-011-0249-8.

Faccenna, C., Piromallo, C., Crespo-Blanc, A., Jolivet, L., and Rossetti, F., 2004, Lateral slab deformation and the origin of the western Mediterranean arcs: Tectonics, v. 23, TC1012, doi: 10.1029/2002TC001488.

Faccenna, C., Becker, T.W., Auer, L., Billi, A., Boschi, L., Brun, J.P., Capitanio, F.A., Funiciello, F., Horvàth, F., Jolivet, L., Piromallo, C., Royden, L., Rossetti, F., and Serpelloni, E., 2014, Mantle dynamics in the Mediterranean: Reviews of Geophysics, v. 52, p. 283–332, doi: 10.1002/2013RG000444.

Fichtner, A., and Villaseñor, A., 2015, Crust and upper mantle of the western Mediterranean - Constraints from full-waveform inversion: Earth and Planetary Science Letters, v. 428, p. 52–62, doi: 10.1016/j.epsl.2015.07.038.

Flecker, R., Krijgsman, W., Capella, W., de Castro Martíns, C., Dmitrieva, E., Mayser, J. P., ... & Tulbure, M., 2015, Evolution of the Late Miocene Mediterranean–Atlantic gateways and their impact on regional and global environmental change: Earth-Science Reviews, v. 150, p. 365-392. doi; 10.1016/j.earscirev.2015.08.007

Frizon de Lamotte, D., Raulin, C., Mouchot, N., Wrobel-Daveau, J.C., Blanpied, C., and Ringenbach, J.C., 2011, The southernmost margin of the Tethys realm during the Mesozoic and Cenozoic: Initial geometry and timing of the inversion processes: Tectonics, v. 30, p. 1-22, doi: 10.1029/2010TC002691.

Galdeano, A., Rossignol, J.C., 1977, Contribution de l'Aeromagnetisme a l'etude du Golfe de

Valence (Mediterranee Occidentale): Earth Planet. Sci. Lett., v. 34, p. 85–99.

Galindo-Zaldivar, J., Gil, A.J., Sanz de Galdeano, C., Lacy, M.C., García-Armenteros, J.A., Ruano, P., Ruiz, A.M., Martínez-Martos, M., and Alfaro, P., 2015, Active shallow extension in central and eastern Betic Cordillera from CGPS data: Tectonophysics, v. 663, p. 290–301, doi: 10.1016/j.tecto.2015.08.035.

Garate, J., Martin-Davila, J., Khazaradze, G., Echeverria, A., Asensio, E., Gil, A.J., de Lacy, M.C., Armenteros, J.A., Ruiz, A.M., Gallastegui, J., Alvarez-Lobato, F., Ayala, C., Rodríguez-Caderot, G., Galindo-Zaldívar, J., et al., 2015, Topo-Iberia project: CGPS crustal velocity field in the Iberian Peninsula and Morocco: GPS Solutions, v. 19, p. 287–295, doi: 10.1007/s10291-014-0387-3.

Garcia-Castellanos, D., Estrada, F., Jiménez-Munt, I., Gorini, C., Fernàndez, M., Vergés, J., and De Vicente, R., 2009, Catastrophic flood of the Mediterranean after the Messinian salinity crisis: Nature, v. 462, p. 778–781, doi: 10.1038/nature08555.

Garcia-Castellanos, D., and Villaseñor, A., 2011, Messinian salinity crisis regulated by competing tectonics and erosion at the Gibraltar arc: Nature, v. 480, p. 359–363, doi: 10.1038/nature10651.

Garcia-Castellanos, D., Micallef, A., Estrada, F., Camerlenghi, A., Ercilla, G., Periáñez, R., Abril, J.M., 2020, The Zanclean megaflood of the Mediterranean - Searching for independent evidence: Earth-Science Reviews 201, 103061.

García-Dueñas, V., Balanyá, J.C., and Martínez-Martínez, J.M., 1992, Miocene extensional detachments in the outcropping basement of the northern Alboran Basin (Betics) and their tectonic implications: Geo-Marine Letters, v. 12, p. 88–95, doi: 10.1007/BF02084917.

Garrido, C.J., Gueydan, F., Booth-Rea, G., Precigout, J., Hidas, K., Padrón-Navarta, J.A., and Marchesi, C., 2011, Garnet lherzolite and garnet-spinel mylonite in the Ronda peridotite: Vestiges of Oligocene back-arc mantle lithospheric extension in the western Mediterranean: Geology, v. 39, p. 927–930, doi: 10.1130/G31760.1.

Gelabert, B., Sàbat, F., and Rodríguez-Perea, A., 2002, A new proposal for the late Cenozoic geodynamic evolution of the western Mediterranean: Terra Nova, v. 14, p. 93–100.

Giaconia, F., Booth-Rea, G., Martínez-Martínez, J.M., Azañón, J.M., Perez-Peña, J.V., Pérez-Romero, J. and Villegas, I., 2012, Geomorphic evidence of active tectonics in the Sierra Alhamilla (eastern Betics, SE Spain): Geomorphology,v. 145-146, p. 90–106.

Giaconia, F., Booth-Rea, G., Martínez-Martínez, J.M., Azañón, J.M., Pérez-Romero, J. and Villegas, I., 2013, Mountain front migration and drainage captures related to fault segment linkage and growth: The Polopos transpressive fault zone (southeastern Betics, SE Spain): Journal of Structural Geology, v. 46, p. 76-91.

Giaconia, F., Booth-Rea, G., Martínez-Martínez, J.M., Azañón, J.M., Storti, F., and Artoni, A., 2014, Heterogeneous extension and the role of transfer faults in the development of the southeastern Betic basins (SE Spain): Tectonics, v. 33, p. 2467–2489, doi: 10.1002/2014TC003681.

Giaconia, F., Booth-Rea, G., Ranero, C.R., Gràcia, E., Bartolome, R., Calahorrano, A., Lo Iacono, C., Vendrell, M.G., Cameselle, A.L., Costa, S., Gómez de la Peña, L., Martínez-Loriente, S., Perea, H., and Viñas, M., 2015, Compressional tectonic inversion of the Algero-Balearic basin: Latemost Miocene to present oblique convergence at the Palomares margin (Western Mediterranean): Tectonics, v. 34, p. 1516–1543, doi: 10.1002/2015TC003861.Gill, R.C.O., Aparicio, A., El Azzouzi, M., Hernandez, J., Thirlwall, M.F., Bourgois, J., and Marriner, G.F., 2004, Depleted arc volcanism in the Alboran Sea and shoshonitic volcanism in Morocco: Geochemical and isotopic constraints on Neogene tectonic processes: Lithos, v. 78, p. 363–388, doi: 10.1016/j.lithos.2004.07.002.

Gómez de la Peña, L., Gràcia, E., Muñoz, A., Acosta, J., Gómez-Ballesteros, M., Ranero, C.R., Uchupi, E., 2016, Geomorphology and Neogene tectonic evolution of the Palomares continental margin (Western Mediterranean). Tectonophysics, v., 689, p. 25–39, doi:10.1016/j.tecto.2016.03.009.

Gómez de la Peña, L., 2017, The origin and tectono-sedimentary structure of the Alboran Basin. Doctoral Thesis, Universidad de Barcelona, 327 pp.

Gómez de la Peña, L., Ranero, C.R., and Gràcia, E., 2018, The Crustal Domains of the Alboran Basin (Western Mediterranean): Tectonics, v. 37, p. 3352–3377, doi: 10.1029/2017TC004946.

Gómez de la Peña, L., Grevemeyer, I., Kopp, H., Díaz, J. Gallart, J., Booth-Rea, G., Gràcia, E., Ranero, C.R., 2020, The lithospheric structure of the Gibraltar Arc System from Wide-Angle Seismic data: Journal of Geophysical Research: Solid Earth. doi: 10.1029/2020JB019854

Gonzalez-Castillo, L., Galindo-Zaldivar, J., de Lacy, M.C., Borque, M.J., Martinez-Moreno, F.J., García-Armenteros, J.A., and Gil, A.J., 2015, Active rollback in the Gibraltar Arc: Evidences from CGPS data in the western Betic Cordillera: Tectonophysics, v. 663, p. 310–321, doi: 10.1016/j.tecto.2015.03.010.

Govers, R., and Wortel, M.J.R., 2005, Lithosphere tearing at STEP faults: response to edges of subduction zones: Earth and Planetary Science Letters, v. 236, Issues 1–2, p. 505-523, ISSN 0012-821X, https://doi.org/10.1016/j.epsl.2005.03.022.

Gràcia, E., Dañobeitia, J., Vergés, J., and Bartolome, R., 2003, Crustal Architecture & Tectonic Evolution of the Gulf of Cadiz (SW Iberian Margin) at the Convergence of the Eurasian & African Plates: Tectonics, v. 22, p. 1–18, doi: 10.1029/2001TC901045.

Gràcia, E., Pallàs, R., Soto, J.I., Comas, M., Moreno, X., Masana, E., Santanach, P., Diez, S., García, M., and Dañobeitia, J., 2006, Active faulting offshore SE Spain (Alboran Sea): Implications for earthquake hazard assessment in the Southern Iberian Margin: Earth and Planetary Science Letters, v. 241, p. 734–749, doi: 10.1016/j.epsl.2005.11.00[illegible].

Gràcia, E., Bartolome, R., Lo Iacono, C., Moreno, X., Stich, D., Martínez-Diaz, J.J., Bozzano, G., Martínez-Loriente, S., Perea, H., Diez, S., Masana, E., Dañobeitia, J.J., Tello, O., Sanz, J.L., et al., 2012, Acoustic and seismic imaging of the Adra Fault (NE Alboran Sea): in search of the source of the 1910 Adra earthquake: Natural Hazards and Earth System Science, v. 12, p. 3255–3267, doi: 10.5194/nhess-12-3255-2012.

Gràcia, E., Grevemeyer, I., Bartolomé, R., Perea, H., Martínez-Loriente, S., Gómez de la Peña, L., Villaseñor, A., Klinger, Y., Lo Iacono, C., Diez, S., Calahorrano, A., Camafort, M., Costa, S., d'Acremont, E., Rabaute, A., Ranero, C.R., 2019, Earthquake crisis unveils the growth of an incipient continental fault system: Nature Communications, 1-11, https://doi.org/10.1038/s41467-019-11064-5.

Grevemeyer, I., Gràcia, E., Villaseñor, A., Leuchters, W., and Watts, A.B., 2015, Seismicity and active tectonics in the Alboran Sea, Western Mediterranean: Constraints from an offshore-onshore seismological network and swath bathymetry data: Journal of Geophysical Research: Solid Earth, v. 120, p. 767–787, doi: 10.1002/2015JB012352.

Grevemeyer, I., Ranero, C.R., and Ivandic, M., 2018, Structure of oceanic crust and serpentinization at subduction trenches: Geosphere, doi:10.1130/GES01537.1.

Gueguen, E., Doglioni, C., and Fernandez, M., 1998, On the post-25 Ma geodynamic evolution of the western Mediterranean: Tectonophysics, v. 298, p. 259–269, doi: 10.1016/S0040-1951(98)00189-9.

Guerra-Merchán, A., Serrano, F., Garcés, M., Gofas, S., Esu, D., Gliozzi, E., and Grossi, F., 2010, Messinian Lago-Mare deposits near the Strait of Gibraltar (Malaga Basin, S Spain): Palaeogeography, Palaeoclimatology, Palaeoecology, v. 285, p. 264–276, doi: 10.1016/j.palaeo.2009.11.019.

Guerrera, F., Martinalgarra, A. and Perrone, V., 1993, Late Oligocene-Miocene Syn/Late-Orogenic Successions in Western and Central Mediterranean Chains from the Betic Cordillera to the Southern Apennines: Terra Nova, v. 5(6), p. 525-544.

Gueydan, F., Mazzotti, S., Tiberi, C., Cavin, R., and Villaseñor, A., 2019, Western Mediterranean Subcontinental Mantle Emplacement by Continental Margin Obduction: Tectonics, v. 38, p. 2142–2157, doi: 10.1029/2018TC005058.

Hidas, K., Konc, Z., Garrido, C.J., Tommasi, A., Vauchez, A., Padron-Navarta, J.A., Marchesi, C., Booth-Rea, G., Acosta-Vigil, A., Szabo, C., Varas-Reus, M.I. and Gervilla, F., 2016, Flow in the western Mediterranean shallow mantle: Insights from xenoliths in Pliocene alkali basalts from SE Iberia (eastern Betics, Spain): Tectonics, v. 35(11), p. 2657-2676.

Hidas, K., Garrido, C. J., Booth-Rea, G., Marchesi, C., Bodinier, J.L., Dautria, J.M., Louni-Hacini, A., and Azzouni-Sekkal, A., 2019, Lithosphere tearing along STEP faults and synkinematic formation of lherzolite and wehrlite in the shallow subcontinental mantle: Solid Earth, v. 10(4), p. 1099-1121.

Hoernle, K., van den Bogaard, P., Duggen, S., Mocek, B., and Garbe-Schönberg, D., 1999, Evidence for Miocene subduction beneath the Alboran Sea: 40Ar/39Ar dating and geochemistry of volcanic rocks from Holes 977A and 978A: Proceedings of the ocean drilling program, v. 161, p. 357–373, doi: 10.2973/odp.proc.sr.161.264.1999.

Hsü, K.J., Cita, M.B., and Ryan, W.B.F., 1973, The origin of the Mediterranean evaporites, in Washington, Printing Office, p. 1203–1231.

Iribarren, L., Vergès, J., Camurri, F., Fullea, J., and Fernández, M., 2007, The structure of the Atlantic-Mediterranean transition zone from the Alboran Sea to the Horseshoe Abyssal Plain (Iberia-Africa plate boundary): Marine Geology, v. 243, p. 97–119, doi: 10.1016/j.margeo.2007.05.011.

Jabaloy-Sánchez, A., Azdimousa, A., Booth-Rea, G., Asebriy, L., Vázquez-Vílchez, M., Martínez-Martínez, J.M., and Gabites, J., 2015, The structure of the Temsamane fold-and-thrust stack (eastern Rif, Morocco): Evolution of a transpressional orogenic wedge: Tectonophysics, v. 663, p. 150–176, doi: 10.1016/j.tecto.2015.02.003.

Jabaloy-Sanchez, A., C. Talavera, M. T. Gomez-Pugnaire, V. Lopez-Sanchez-Vizcaino, M. Vazquez-Vilchez, M. J. Rodriguez-Peces, and N. J. Evans, 2018, U-Pb ages of detrital zircons from the Internal Betics: A key to deciphering paleogeographic provenance and tectono-stratigraphic evolution: Lithos, v. 318, p. 244-266.

Johnson, C., N. Harbury, and A. J. Hurford, 1997, The role of extension in the Miocene denudation of the Nevado-Filábride Complex, Betic Cordillera (SE Spain): Tectonics, v. 16(2), p. 189–204, doi:10.1029/96TC03289.

Jolivet, L., Frizon de Lamotte, D., Mascle, A., and Seranne, M., 1999, The Mediterranean Basins: Tertiary Extension within the Alpine Orogen - an introduction: Geological Society, London, Special Publications, v. 156, p. 1–14, doi: 10.1144/GSL.SP.1999.156.01.02.

Jolivet, L., Faccenna, C., and Piromallo, C., 2009, From mantle to crust: Stretching the Mediterranean: Earth and Planetary Science Letters, v. 285, p. 198–209, doi: 10.1016/j.epsl.2009.06.017.

Jolivet, L., and Faccenna, C., 2000, Mediterranean extension and the Africa-Eurasia collision: Tectonics, v. 19, p. 1095–1106.Juan, C., Ercilla, G., Javier Hernández-Molina, F., Estrada, F., Alonso, B.,

Casas, D., García, M., Farran, M., Llave, E., Palomino, D., Vázquez, J.T., Medialdea, T., Gorini, C., D'Acremont, E., et al., 2016, Seismic evidence of current-controlled sedimentation in the Alboran Sea during the Pliocene and Quaternary: Palaeoceanographic implications: Marine Geology, doi: 10.1016/j.margeo.2016.01.006.

Jurado, M.J., and Comas, M.C., 1992, Well log interpretation and seismic character of the Cenozoic sequence in the norhtern Alboran Sea: Geo-Marine Letters, v. 12, p. 129–136.

Kirchner, K. L., Behr, W. M., Loewy, S., and Stockli, D. F., 2016, Early Miocene subduction in the western Mediterranean: Constraints from Rb-Sr multimineral isochron geochronology: Geochemistry, Geophysics, Geosystems, v. 17(5), p. 1842-1860.

Krijgsman, W., Garces, M., Agusti, J., Raffi, I., Taberner, C. and Zachariasse, W.J., 2001. The 'Tortonian salinity crisis' of the eastern Betics (Spain): Earth and Planetary Science Letters, v. 181(4), p. 497-511.

Lafosse, M., d'Acremont, E., Rabaute, A., Mercier de Lépinay, B., Tahayt, A., Ammar, A., and Gorini, C., 2016, Evidence of quaternary transtensional tectonics in the Nekor basin (NE Morocco): Basin Research, p. 1–20, doi: 10.1111/bre.12185.

Leprêtre, A., Klingelhoefer, F., Graindorge, D., Schnurle, P., Beslier, M.O., Yelles, K., Déverchère, J., and Bracene, R., 2013, Multiphased tectonic evolution of the Central Algerian margin from combined wide-angle and reflection seismic data off Tipaza, Algeria: Journal of Geophysical Research: Solid Earth, v. 118, p. 3899–3916, doi: 10.1002/jgrb.50318.

Levander, A, Bezada, M.J., Niu, F., Humphreys, E.D., Palomeras, I., Thurner, S.M., Masy, J., Schmitz, M., Gallart, J., Carbonell, R., and Miller, M.S., 2014, Subduction-driven recycling of continental margin lithosphere: Nature, v. 515, p. 253–256, doi: 10.1038/nature13878.

Lofi, J., Déverchère, J., Gorini, C., Gaullier, V., Giller, H., Guennoc, P., Loncke, L., Maillard, A., Sage, F., and Thinon, I., 2011, Atlas of the Messinian Salinity Crisis markers in the Mediterranean and Black Seas.: Seas Mémoires de la Société géologique de Frace 179. World Geological Map Commission, 72 p.

Lonergan, L. and Mangerajetzky, M.A., 1994, Evidence for Internal Zone Unroofing from Foreland Basin Sediments, Betic Cordillera, Se Spain: Journal of the Geological Society, v. 151, p. 515-529.

Lonergan, L., and White, N., 1997, Origin of the Betic-Rif mountain belt: Tectonics, v. 16, p. 504–522.

Lonergan L, and Johnson C, 1998, Reconstructing orogenic exhumation histories using synorogenic detrital zircons and apatites: an example from the Betic Cordillera, SE Spain, Basin Research, v. 10, p. 353-364, ISSN: 0950-091X

López-Rodríguez, C., De Lange, G.J., Comas, M., Martínez-Ruiz, F., Nieto, F., Sapart, C.J., and Mogollón, J.M., 2019, Recent, deep-sourced methane/mud discharge at the most active mud volcano in the western Mediterranean: Marine Geology, v. 408, p. 1–17, doi: 10.1016/j.margeo.2018.11.013.

López Sánchez-Vizcaíno, V., D. Rubatto, M. T. Gómez-Pugnaire, V. Trommsdorff, and O. Müntener, 2001, Middle Miocene high-pressure metamorphism and fast exhumation of the Nevado-Filábride complex, SE Spain: Terra Nova, v. 13, p. 327-332.

Luján, M., Crespo-Blanc, A. and Balanya, J.C., 2006, The Flysch Trough thrust imbricate (Betic Cordillera): A key element of the Gibraltar Arc orogenic wedge: Tectonics, v. 25(6), TC6001; doi:10.1029/2005TC001910.

Lustrino, M., Duggen, S., and Rosenberg, C.L., 2011, The Central-Western Mediterranean: Anomalous igneous activity in an anomalous collisional tectonic setting: Earth-Science Reviews, v. 104, p. 1–40, doi: 10.1016/j.earscirev.2010.08.002.

Mancilla, F. de L., Booth-Rea, G., Stich, D., Pérez-Peña, J.V., Morales, J., Azañón, J.M., Martin, R., and Giaconia, F., 2015, Slab rupture and delamination under the Betics and Rif constrained from receiver functions: Tectonophysics, v. 663, p. 225–237, doi: 10.1016/j.tecto.2015.06.028.

Mancilla, F. de L., and Diaz, J., 2015, High resolution Moho topography map beneath Iberia and Northern Morocco from receiver function analysis: Tectonophysics, v. 663, p. 203–211, doi: 10.1016/j.tecto.2015.06.017.

Marchesi, C., Garrido, C.J., Bosch, D., Bodinier, J.L., Hidas, K., Padrón-Navarta, J.A., and Gervilla, F., 2012, A Late Oligocene Suprasubduction Setting in the Westernmost Mediterranean Revealed by Intrusive Pyroxenite Dikes in the Ronda Peridotite (Southern Spain): The Journal of Geology, v. 120, p. 237–247, doi: 10.1086/663875.

Martín, J. M., J. C. Braga, and C. Betzler, 2003, Late Neogene-recent uplift of the Cabo de Gata volcanic province, Almeria, SE Spain: Geomorphology, v. 50(1-3), p. 27–42, doi:10.1016/S0169-555X(02)00206-4.

Martín-Martín, M., and Martín-Algarra, A., 2002, Thrust sequence and syntectonic sedimentation in a piggy-back basin: the Oligo-Aquitanian Mula–Pliego Basin (Internal Betic Zone, SE Spain): Comptes Rendus Geoscience, v. 334(5), p. 363-370.

Martínez del Olmo, W., and Comas, C., 2008, Arquitectura sismica, olistrostomas y fallas extensionales en el Norte de la Cuenca Oeste del Mar de Alborán: Revista de la Sociedad Geologica de España, v. 21, p. 151–167.

Martínez-García, P., Soto, J.I., and Comas, M., 2011, Recent structures in the Alboran Ridge and Yusuf fault zones based on swath bathymetry and sub-bottom profiling: Evidence of active tectonics: Geo-Marine Letters, v. 31, p. 19–36, doi: 10.1007/s00367-010-0212-0.

Martínez-García, P., Comas, M., Soto, J.I., Lonergan, L., and Watts, A. B., 2013, Strike-slip tectonics and basin inversion in the Western Mediterranean: the Post-Messinian evolution of the Alboran Sea: Basin Research, v. 25, p. 361–387, doi: 10.1111/bre.12005.

Martínez-García, P., Comas, M., Lonergan, L., and Watts, A.B., 2017, From extension to shortening: tectonic inversion distributed in time and space in the Alboran Sea, Western Mediterranean: Tectonics, doi: 10.1002/2017TC004489.

Martínez-Loriente, S., Sallarès, V., Gràcia, E., Bartolome, R., Dañobeitia, J.J., and Zitellini, N., 2014, Seismic and gravity constraints on the nature of the basement in the Africa-Eurasia plate boundary: New insights for the geodynamic evolution of the SW Iberian margin: Journal of Geophysical Research: Solid Earth, p. 127–149, doi: 10.1002/2013JB010601.

Martínez-Martínez, J.M., Soto, J.I. and Balanya, J.C., 2002, Orthogonal folding of extensional detachments: Structure and origin of the Sierra Nevada elongated dome (Betics, SE Spain): Tectonics,v. 21(3), p 1-20, doi: 10.1029/2001TC001283.

Martínez-Martínez, J.M., Booth-Rea, G., Azañón, J.M. and Torcal, F., 2006, Active transfer fault zone linking a segmented extensional system (Betics, southern Spain): Insight into heterogeneous extension driven by edge delamination. Tectonophysics, 422(1-4): 159-173.

Mauffret, A., Frizon de Lamotte, D., Lallemant, S., Gorini, C., and Maillard, A., 2004, E-W opening of the Algerian Basin (Western Mediterranean): Terra Nova, v. 16, p. 257–264, doi: 10.1111/j.1365-3121.2004.00559.x.

Maury, R., Fourcade, S., Coulon, C., El Azzouzi, M., Bellon, H., Coutelle, A., Ouabadi, A., Semroud, B., Megartsi, M., Cotten, J., Belanteur, O., Louni-Hacini, A., Piqué, A., Capdevila, R., et al., 2000, Post-collisional Neogene magmatism of the Mediterranean Maghreb margin: A consequence of slab breakoff: Comptes Rendus de l'Academie de Science - Serie IIa: Sciences de la Terre et des Planetes, v. 331, p. 159–173, doi: 10.1016/S1251-8050(00)01406-3.

Mazzoli, S., and Helman, M., 1994, Neogene patterns of relative plate motion for Africa-Europe: some implications for recent central Mediterranean tectonics: Geologische Rundschau, v. 83, p. 464–468, doi: 10.1007/BF00210558.

Medaouri, M., Bracene, R., Deverchere, J., Graindorge, D., Ouabadi, A., and Yelles-Chaouche, A.K., 2012, Structural styles and neogene petroleum system around the Yusuf-Habibas ridge (Alboran basin, Mediterranean sea): The Leading Edge, v. Special, p. 776–785.

Medaouri, M., Déverchère, J., Graindorge, D., Bracene, R., Badji, R., Ouabadi, A., Yelles-Chaouche, K., and Bendiab, F., 2014, The transition from Alboran to Algerian basins (Western Mediterranean Sea): Chronostratigraphy, deep crustal structure and tectonic evolution at the rear of a narrow slab rollback system: Journal of Geodynamics, v. 77, p. 186–205, doi: 10.1016/j.jog.2014.01.003.

Medina, F., and Cherkaoui, T. E., 2017, The South-Western Alboran Earthquake Sequence of January-March 2016 and Its Associated Coulomb Stress Changes: Open Journal of Earthquake Research, v. 06, p. 35–54, doi: 10.4236/ojer.2017.61002.

Merino I., Prada M., Ranero C. R., Sallarès V., Aslanian D., Schnurle P., 2019, The crustal structure of the continent-ocean transition along the Gulf of Lions from Travel-Time Tomography of MCS and WAS data. Abstract [T33G-0448] 2019 Fall Meeting, AGU, San Francisco, CA, 9-13 Dec.

Michard, A., A. Mokhtari, P. Lach, P. Rossi, A. Chalouan, O. Saddiqi, and E. C. Rjimati, 2018, Liassic age of an oceanic gabbro of the External Rif (Morocco): Implications for the Jurassic continent-ocean boundary of Northwest Africa, Cr Geosci, v. 350(6), p. 299-309.

Montenat, C., and P. Ott d'Estevou, 1990, Easten betic Neogene Basins—A review, in Les Bassins Neogenes du Domaine Bétique Orientale (Espagne), Documents et Travaux, edited by C. Montenat, p. 9–15, IGAL, Paris.

Moreno, X., Gràcia, E., Bartolomé, R., Martínez-Loriente, S., Perea, H., Gómez de la Peña, L., Iacono, C. Lo, Piñero, E., Pallàs, R., Masana, E., and Dañobeitia, J.J., 2016, Seismostratigraphy and tectonic architecture of the Carboneras Fault offshore based on multiscale seismic imaging: Implications

for the Neogene evolution of the NE Alboran Sea: Tectonophysics, v. 689, p. 115–132, doi: 10.1016/j.tecto.2016.02.018.

Negro, F., de Sigoyer, F., Goffé, B., Saddiqi, O., and Villa, I.M., 2008, Tectonic evolution fo the Betic-Rif arc: New constraints from 40Ar/39Ar dating on white micas in the Temsamane units (External Rif, northern Morocco): Lithos, v. 106, p. 93–109, doi: 10.1016/j.lithos.2008.06.011.

Nocquet, J.M., 2012, Present-day kinematics of the Mediterranean: A comprehensive overview of GPS results: Tectonophysics, v. 579, p. 220–242, doi: 10.1016/j.tecto.2012.03.037.

Ott d'Estevou, P. and Montenant, 1990, Le Basin de Sorbas-Tabernas. In: C. Montenant (Editor), Les bassins neogenes du domaine Bétique oriental (Espagne). Doc. et trav. IGAL, CNRS, Paris, pp. 101-128.

Palano, M., González, P.J., and Fernández, J., 2015, The Diffuse Plate boundary of Nubia and Iberia in the Western Mediterranean: Crustal deformation evidence for viscous coupling and fragmented lithosphere: Earth and Planetary Science Letters, v. 430, p. 439–447, doi: 10.1016/j.epsl.2015.08.040.

Palomino, D., Vázquez, J.T., Ercilla, G., Alonso, B., López-González, N., and Díaz-del-Río, V., 2011, Interaction between seabed morphology and water masses around the seamounts on the Motril Marginal Plateau (Alboran Sea, Western Mediterranean): Geo-Marine Letters, v. 31, p. 465–479, doi: 10.1007/s00367-011-0246-y.

Platt, J.P., and Vissers, R.L.M., 1989, Extensional collapse of thikened continental lithosphere: A working hipothesis for the Alboran Sea and Gibraltar Arc: Geology, v. 17, p. 540–543.

Platt, J.P., Whitehouse, M.J., Kelley, S.P., Carter, A., Hollick, L., 2003, Simultaneous extensional exhumation across the Alboran Basin: Implications for the causes of late orogenic extension. Geology 31, 251–254.

Platt, J.P., Kelley, S.P., Carter, A., and Orozco, M., 2005, Timing of tectonic events in the Alpujárride Complex, Betic Cordillera, southern Spain: Journal of Geological Society, London, v. 162, p. 451–462.

Platt, J. P., R. Anczkiewicz, J. I. Soto, S. P. Kelley, and M. Thirlwall, 2006, Early Miocene continental subduction and rapid exhumation in the western Mediterranean: Geology, v. 34(11), p. 981-984.

Platt, J.P., Behr, W.M., Johanesen, K., and Williams, J.R., 2013, The Betic-Rif Arc and Its Orogenic Hinterland: A Review: Annual Review of Earth and Planetary Sciences, v. 41, p. 313–357, doi: 10.1146/annurev-earth-050212-123951.

Prada, M., Ranero, C.R., Sallares, V., Grevemeyer, I., de Franco, R., Gervasi, A., Zitellini, N., 2020, The structure of Mediterranean arcs: New insights from the Calabrian Arc subduction system: Earth and Planetary Science Letters, v.548, 116480, https://doi.org/10.1016/j.epsl.2020.116480.

Prada, M., Sallares, V., Ranero, C.R., Vendrell, M.G., Grevemeyer, I., Zitellini, N., and de Franco, R., 2015, The complex 3D transition from continental crust to back-arc magmatism and exhumed mantle in the Central Tyrrhenian basin: Geophys. J. International., v.203, p. 63-78, doi: 10.1093/gji/ggv271.

Prada, M., Sallares, V., Ranero, C.R., Vendrell, M.G., Grevemeyer, I., Zitellini, N., and de Franco, R., 2014, Seismic structure of the Central Tyrrhenian basin: Geophysical constraints on the nature of the main crustal domains: J. Geophys. Res. Solid Earth, v. 119, doi:10.1002/2013JB010527.

Ranero C.R., Reston T.J., Belykh I., Gnibidenko H., 1997a, Reflective oceanic crust formed at a fast-spreading center in the Pacific: Geology, v.25, pp499-502.

Ranero CR, Banda E, Buhl P., 1997b, The crustal structure of the Canary Basin: Accretion processes at slow spreading centers: Journal Of Geophysical Research-Solid Earth, v. 102, p. 10185-10201.

Ranero, C.R., Von Huene, R., Flueh, E., Duarte, M., Baca, D., and McIntosh, K., 2000, A cross section of the convergent Pacific margin of Nicaragua: Tectonics, v. 19, p. 335–357, doi: 10.1029/1999TC900045.Rehault, J.P., Boillot, G., and Mauffret, A., 1984, The Western Mediterranean Basin geological evolution: Marine Geology, v. 55, p. 447–477, doi: 10.1016/0025-3227(84)90081-1.

Rodríguez-Fernández, J.R. and Sanz de Galdeano, C., 1992, Onshore Neogene stratigraphy in the North of the Alboran Sea (Betic Internal Zones): Paleogeographic implications: Geo-Marine Letters, v. 12, p. 123-128. doi: 10.1007/BF02084922

Rodriguez-Fernández, J., Comas, M., Soria, J., Martín-Pérez, J.A., Soto, J.I., 1999, The sedimentary record of the Alborán basin: An attempt at sedimentary sequence correlation and subsidence analysis: Proc. Ocean Drill. Program Sci. Results 161, 69-76.

Rodríguez-Fernández, J., Azor, A. and Miguel Azañón, J., 2011. The Betic Intramontane Basins (SE Spain): Stratigraphy, Subsidence, and Tectonic History, Tectonics of Sedimentary Basins. John Wiley & Sons, Ltd, pp. 461-479

Rodríguez-Fernández, J, Azor, A. and Miguel Azañón, J., 2012, The Betic Intramontane Basins (SE Spain): Stratigraphy, Subsidence, and Tectonic History. In Tectonics of Sedimentary Basins (eds C. Busby and A. Azor). doi:10.1002/9781444347166.ch23

Rohling, E.J., Schiebel, R., and Siddall, M., 2008, Controls on Messinian Lower Evaporite cycles in the Mediterranean: Earth and Planetary Science Letters, v. 275, p. 165–171, doi: 10.1016/j.epsl.2008.08.022.

Rosenbaum, G., Lister, G.S., and Duboz, C., 2002, Reconstruction of the tectonic evolution of the western Mediterranean since the Oligocene: Journal of the Virtual Explorer, v. 8, p. 107–126.

Rouchy, J.M., and Caruso, A., 2006, The Messinian salinity crisis in the Mediterranean basin: A reassessment of the data and an integrated scenario: Sedimentary Geology, v. 188–189, p. 35–67, doi: 10.1016/j.sedgeo.2006.02.005.

Rovere, M.; Ranero, C. R., Sartori, R., Torelli, L., Zitellini, N., 2004, Seismic images and magnetic signature of the Late Jurassic to Early Cretaceous Africa–Eurasia plate boundary off SW Iberia: Geophysical Journal International, v. 158, p. 554–568.

Roveri, M., Flecker, R., Krijgsman, W., Lofi, J., Lugli, S., Manzi, V., Sierro, F.J., Bertini, A., Camerlenghi, A., De Lange, G., Govers, R., Hilgen, F.J., Hübscher, C., Th Meijer, P., et al., 2014, The Messinian Salinity Crisis: Past and future of a great challenge for marine sciences: Marine Geology, v. 352, p. 25–58, doi: 10.1016/j.margeo.2014.02.002.

Royden, L.H., 1993, Evolution of retreating subduction boundaries formed during continental collision: Tectonics, v. 12, p. 629–638, doi: 10.1029/92TC02641.

Ruegg, G., 1964, Geologische onderzoekingen in het bekken van Sorbas, S Spanje. Amsterdan Geological Institute, Univ. of Amsterdan, 64 pp.

Sallarès, V., Gailler, A., Gutscher, M.A., Graindorge, D., Bartolomé, R., Gràcia, E., Díaz, J., Dañobeitia, J.J., and Zitellini, N., 2011, Seismic evidence for the presence of Jurassic oceanic crust in the central Gulf of Cadiz (SW Iberian margin): Earth and Planetary Science Letters, v. 311, p. 112–123, doi: 10.1016/j.epsl.2011.09.003.

Sallarès, V., Martínez-Loriente, S, Prada, M., Gràcia, E., Ranero, C.R., Gutscher, MA., Bartolome, R., Gailler, A., Danobeitia, J.J., Zitellini, N., 2013, Seismic evidence of exhumed mantle rock basement at the Gorringe Bank and the adjacent Horseshoe and Tagus abyssal plains (SW Iberia): Earth and Planetary Science Letters, v. 365, p. 120–131.

Sánchez Rodríguez, L., Gebauer, D., 2000, Mesozoic Formation of Pyroxenites and Gabbros in the Ronda Area (Southern Spain), Followed by Early Miocene Subduction Metamorphism and Emplacement into the Middle Crust - U-Pb Sensitive High-Resolution Ion Microprobe Dating of Zircon: Tectonophysics v. 316, p. 19-44.

Sanz De Galdeano, C., 1990, Geologic evolution of the Betic Cordilleras in the Western Mediterranean, Miocene to the present: Tectonophysics, v. 172, p. 107–119, doi: 10.1016/0040-1951(90)90062-D.

Sartori, R., Torelli, L., Zitellini, N., Peis, D. and Lodolo, E., 1994, Eastern segment of the Azores-Gibraltar line (central-eastern Atlantic): An oceanic plate boundary with diffuse compressional deformation, Geology, v. 22, p. 555–558.

Sautkin, A., Talukder, A.R., Comas, M.C., Soto, J.I, and Alekseev, A., 2003, Mud volcanoes in the Alboran Sea: evidence from micropaleontological and geophysical data, Mar Geol, v. 195(1-4), p. 237-261.

Schettino, A., and Turco, E., 2011, Tectonic history of the western Tethys since the Late Triassic: Geological Society of America Bulletin, v. 123, p. 89–105, doi: 10.1130/B30064.1.

Seber, D., Barazangi, M., Ibenbrahim, A., and Demnati, A., 1996, Geophysical evidence for lithospheric delamination beneath the alboran Sea and Rif-Betic mountains: Nature, v. 379, p. 6.

Serrano, F., Guerra-Merchan, A., El Kadiri, K., de Galdeano, C.S., Lopez-Garridoc, A.C., Martin-Martin, M. and Hlila, R., 2007, Tectono-sedimentary setting of the oligocene-early Miocene deposits on the betic-rifian internal zone (Spain and Morocco): Geobios, v. 40(2), p. 191-205.

Serrano, F., Sanz De Galdeano, C., El Kadiri, K., Guerra-Merchan, A., Lopez-Garrido, A.C., Martin-Martin, M., and Hlila, R., 2006, Oligocene-early Miocene transgressive cover of the Betic-Rif Internal Zone. Revision of its geologic significance: Eclogae Geol Helv, v. 99(2), p. 237-253.

Somoza, L., Medialdea, T., León, R., Ercilla, G., Vázquez, J.T., Farran, M., Hernández-Molina, J., González, J., Juan, C., and Fernández-Puga, M.C., 2012, Structure of mud volcano systems and pockmarks in the region of the Ceuta Contourite Depositional System (Western Alboran Sea): Marine Geology, v. 332–334, p. 4–26, doi: 10.1016/j.margeo.2012.06.002.

Soria, J.M., Fernandez, J., Viseras, C., 1999, Late Miocene stratigraphy and palaeogeographic evolution of the intramontane Guadix Basin (Central Betic Cordillera, Spain): implications for an Atlantic-Mediterranean connection: Palaeogeogr Palaeocl 151, 255-266.

Soto, J.I., Fernández-Ibáñez, F., Talukder, A.R., and Martínez-García, P., 2010, Miocene Shale Tectonics in the Northern Alboran Sea (Western Mediterranean): AAPG Memories, v. 93, p. 119–144, doi: 10.1306/13231312M933422.

Soto, J.I., Fernández-Ibáñez, F., and Talukder, A.R., 2012, Recent shale tectonics and basin evolution of the NW Alboran Sea: The Leading Edge, p. 768–775.

Spakman, W., and Wortel, R., 2004, A tomographic view on Western Mediterranean Geodynamics: The TRANSMED Atlas, The Mediterranean Region from Crust to Mantle, p. 31–52, doi: 10.1007/978-3-642-18919-7_2.

Spakman, W., Chertova, M. V., Van Den Berg, A., and van Hinsbergen, D.J.J., 2018, Puzzling features of western Mediterranean tectonics explained by slab dragging: Nature Geoscience, v. 11, p. 211–216, doi: 10.1038/s41561-018-0066-z.

Strzerzynski, P., Déverchère, J., Cattaneo, A., Domzig, A., Yelles, K., De Lépinay, B.M., Babonneau, N., and Boudiaf, A., 2010, Tectonic inheritance and Pliocene-Pleistocene inversion of the Algerian margin around Algiers: Insights from multibeam and seismic reflection data: Tectonics, v. 29, doi: 10.1029/2010TC002716.

Torelli, L., Sartori, R., and Zitellini, N., 1997, The giant chaotic body in the Atlantic Ocean off Gibraltar: New results from a deep seismic reflection survey: Marine and Petroleum Geology, v. 14, p. 125–134, doi: 10.1016/S0264-8172(96)00060-8.

Torres-Roldan, R.L., Poli, G., and Peccerillo, A., 1986, An early Miocene arc-tholeitic magmatic dyke event from the Alboran sea: Evidence for precollision subduction and back-arc crustal extension in the westernmost Mediterranean: Geologische Rundschau, v. 75, p. 219–234.

Turner, S. P., J. P. Platt, R. M. M. George, S. P. Kelley, D. G. Pearson, and G. M. Nowell, 1999, Magmatism Associated with Orogenic Collapse of the Betic-Alboran Domain, Se Spain, J. Petrol., v. 40(6), p. 1011-1036.

van Hinsbergen, D.J.J., Vissers, R.L.M., and Spakman, W., 2014, Origin and consequences of western Mediterranean subduction, rollback, and slab segmentation: Tectonics, v. 33, p. 393–419, doi: 10.1002/2013TC003349.

van Hinsbergen, D.J.J., Torsvik, T.H., Schmid, S.M., Matenco, L.C., Maffione, M., Vissers, R.L.M., Gürer, D., Spakman, W., 2020, Orogenic architecture of the Mediterranean region and kinematic reconstruction of its tectonic evolution since the Triassic: Gondwana Research v. 81, p. 79-229.

Varas-Reus, M.I., Garrido, C.J., Marchesi, C., Bosch, D., Acosta-Vigil, A., Hidas, K., Barich, A., and Booth-Rea, G., 2017, Sr-Nd-Pb isotopic systematics of crustal rocks from the western Betics (S. Spain): Implications for crustal recycling in the lithospheric mantle beneath the westernmost Mediterranean: Lithos, v. 276, p. 45–61, doi: 10.1016/j.lithos.2016.10.003.

Vázquez, M., Jabaloy, A., Barbero, L., and Stuart, F.M., 2011, Deciphering tectonic- and erosion-driven exhumation of the Nevado-Filábride Complex (Betic Cordillera, Southern Spain) by low

temperature thermochronology: Terra Nova, v. 23(4), p. 257–263, doi:10.1111/ j.1365-3121.2011.01007.x.

Vergés, J., and Fernàndez, M., 2012, Tethys-Atlantic interaction along the Iberia-Africa plate boundary: The Betic-Rif orogenic system: Tectonophysics, v. 579, p. 144–172, doi: 10.1016/j.tecto.2012.08.032.

Vissers, R.L.M., Platt, P., and van der Wal, D., 1995, Late orogenic extension of the Betic Cordillera and the Alboran Domain: A lithosphecir view: Tectonics, v. 14, p. 786–803, doi: 10.1029/95TC00086.

Völk, H.R., 1967, Zur Geologie und stratigraphie des Neogenbeckens von Vera, SüdostSpanien. Ph.D. Thesis, Municipal University of Amsterdam, Netherlands.

Watts, A.B., Platt, J.P., and Buhl, P., 1993, Tectonic evolution of the Alboran Sea basin: Basin Research, v. 5, p. 153–177.

Wessel, P., and Smith, W.H.F., 1991, Free software helps map and display data: Eos, Transactions American Geophysical Union, v. 72, p. 441–446, doi: 10.1029/90EO00319.

Wortel, M.J., and Spakman, W., 2000, Subduction and slab detachment in the Mediterranean-Carpathian region: Science (New York, N.Y.), v. 290, p. 1910–1917, doi: 10.1126/science.290.5498.1910.

Zeck, H.P., 1999, Alpine plate kinematics in the western Mediterranean: a westward-directed subduction regime followed by slab roll-back and slab detachment: Geological Society, London, Special Publications, v. 156, p. 109–120, doi: 10.1144/GSL.SP.1999.156.01.07.

Zeck, H. P., Maluski, H., and Kristensen, A. B., 2000, Revised geochronology of the Neogene calc-alkaline volcanic suite in Sierra de Gata, Alborán volcanic province, SE Spain: Journal of the Geological Society, v.157(1), p. 75-81.

Zitellini, N., Gràcia, E., Matias, L., Terrinha, P., Abreu, M.A., De Alteriis, G., Henriet, J.P., Dañobeitia, J.J., Masson, D.G., Mulder, T., Ramella, R., Somoza, L., and Diez, S., 2009, The quest for the Africa-Eurasia plate boundary west of the Strait of Gibraltar: Earth and Planetary Science Letters, v. 280, p. 13–50, doi: 10.1016/j.epsl.2008.12.005.

Zitellini, N., Ranero, C. R., Loreto, M. F., Ligi, M., Pastore, M., Doriano, F., Sallares, V., Grevemeyer, I., Moeller, S., Prada, M., 2020, Recent inversion of the Tyrrhenian Basin. Geology, Geology, v. 48, p. 123–127, https://doi.org/10.1130/G46774.1

Declaration of interests

☒ The authors declare that they have no known competing financial interests or personal relationships that could have appeared to influence the work reported in this paper.

☐The authors declare the following financial interests/personal relationships which may be considered as potential competing interests: